

AD716803

**ELECTRONIC SIGNAL PROCESSING
TECHNIQUES**

NONDESTRUCTIVE TESTING

PHASE II

ANNUAL REPORT

NOVEMBER 1970

Reproduced by
NATIONAL TECHNICAL
INFORMATION SERVICE
Springfield, Va 22151

THE **BOEING** COMPANY
SEATTLE WASHINGTON

**BEST
AVAILABLE COPY**

ELECTRONIC SIGNAL PROCESSING TECHNIQUES
PHASE II - NONDESTRUCTIVE TESTING

by

JAMES C. KENNEDY
and
WAYNE E. WOODMANSEE

Annual Report
30 October 1969 to 29 October 1970

Contract Number DAAA 25-69-C0206

Sponsored by
Advanced Research Projects Agency
Department of Defense, Washington, D. C.
ARPA Order No. 1246

Monitored by
FRANKFORD ARSENAL
Philadelphia, Pennsylvania

The Boeing Company
Seattle, Washington 98124

November 1970

This document has been approved
for release and sale; its
distribution is unlimited.

FOREWORD

This report was prepared by The Boeing Company, Aerospace Group, Seattle, Washington under Contract DAAA 25-69-C0206 and covers the work performed between October 1969 and October 1970. This is the final report for Phase II of Electronic Signal Processing Techniques. Phase I was conducted between October 1968 and July 1969.

The program is sponsored by the Advanced Research Projects Agency of the Department of Defense under ARPA Order 1246, Program Element Code G1101D. The program is being administered under the direction of the Frankford Arsenal by Mr. Eugene Roffman.

The program is being conducted at The Boeing Company, Kent Space Center Materials and Processes Laboratory. Mr. Howard A. Johnson is the Program Manager, Dr. Wayne E. Woodmansee is the Technical Leader, and Mr. James C. Kennedy is the Principal Investigator.

ABSTRACT

Signal averaging was used to enhance flaw indications in the ultrasonic inspection of electron beam welds. An electronic gate, synchronized to the transducer motion through the use of an electrically controllable delay was also used to enhance flaw indications. To aid in electronic signal processing, a technique for recording ultrasonic video information on a low-frequency tape recorder was developed. In preparation for optical matched filtering, ultrasonic information was recorded on a photographic transparency in a C-scan format. An XY scanning densitometer was constructed to remove the intensity modulated information from the film and to aid in the production of hard copy recordings. Phaselock detection was used to perform through transmission eddy current testing. Methods were developed for obtaining quantitative through transmission data. Through transmission thickness measurements were performed and procedures were developed for obtaining a linear relationship between part thickness and eddy current signal. Applications to chemical milling and in-motion thickness measurements were demonstrated. Phaselock detection and signal averaging were used to measure resistance and inductance changes in conventional eddy current coils during a scanning operation. Quantitative data was produced from bridge unbalance signals. The data has the form X/X_0 vs. $\Delta R/X_0$. An application to aluminum brazed titanium honeycomb was examined. Phaselock detection and signal averaging were used to produce quantitative data in two coil eddy current systems. The data has the form V_{in}/V_0 vs. V_{quad}/V_0 . An application to the inspection of ferrous materials was examined.

TABLE OF CONTENTS

	<u>Page</u>
INTRODUCTION	1
DISCUSSION	2
Signal Averaging in Ultrasonic Weld Inspection	2
Ultrasonic Weld Inspection With a Moving Gate	3
Tape Recorded Ultrasonic Information	8
Film Recorded Ultrasonic Information and Optical Processing	17
Eddy Current Through Transmission Testing	25
Through Transmission Thickness Measurement Applications	34
Chemical Milling Thickness Monitor	34
Ribbon Thickness Monitor	38
Phase Sensitive Eddy Current Testing Applied to Bolt Hole Crack Detection	41
Quantitative Eddy Current Testing	52
Single Coil Tests	52
Double Coil Tests	62
SUMMARY	72
FUTURE WORK	73
ACKNOWLEDGEMENTS	74
REFERENCES	75

LIST OF ILLUSTRATIONS

	<u>Page</u>
1. Equipment for Signal Averaging in Ultrasonic Weld Inspection	4
2. Test Specimen and Transducer for Ultrasonic Weld Inspection	5
3. Electronics for Signal Averaging in Ultrasonic Weld Inspection	6
4. Signal Averaging Data	7
5. Electronics for Weld Inspection with a Moving Gate	9
6. Moving Gate Data	10
7. Equipment for Tape Recording Ultrasonic Information	12
8. Electronics for Tape Recorded Ultrasound-Record Mode	13
9. Electronics for Tape Recorded Ultrasound-Playback Mode	15
10. Test Part Used for Tape Recording Ultrasonic Flaw Indications	16
11. Storage Oscilloscope Display of Tape Recorded Ultrasonic Information	16
12. Storage Oscilloscope Display of Tape Recorded Ultrasonic Flaw Indications	18
13. Optical Processing of Ultrasonic Information	19
14. Electronics for Film Recording Ultrasonic Information	21
15. Equipment for Film Recording Ultrasonic Information	22
16. X-Y Scanning Densitometer	23
17. Calibration Curve for Film Recording Ultrasonic Information	24
18. Film Recorded Ultrasonic Flaw Indications	24
19. Conventional "A" Scan Recording of Ultrasonic Flaw Indications	26
20. "A" Scan Produced from Film Recorded Flaw Indications	26
21. Circuitry for Through Transmission Eddy Current Testing	28
22. Through Transmission Eddy Current Data	29
23. Parametric Plot of Through Transmission Eddy Current Data	30
24. Through Transmission Eddy Current Data in Terms of Frequency Thickness Product — V_{in} vs. (ft)	32
25. Through Transmission Eddy Current Data in Terms of Frequency Thickness Product — V_{quad} vs. (ft)	33

	<u>Page</u>
26. Through Transmission Data Compared With Theory	35
27. Apparatus for Chemical Milling Thickness Monitor	36
28. Test Coil Arrangement for Chemical Milling Thickness Monitor	37
29. Calibration Curve for Chemical Milling Process Monitor	39
30. Titanium Chemical Milling Thickness Data	39
31. Part Position Sensitivity	40
32. Equipment for Ribbon Thickness Monitor	42
33. Apparatus for Ribbon Thickness Monitor	43
34. Calibration Curve for Ribbon Thickness Measurement	44
35. Titanium Ribbon Thickness Data	44
36. Block Diagram of Bolt Hole Crack Detection Equipment	46
37. Apparatus for Bolt Hole Crack Detection	47
38. Probe and Test Part for Bolt Hole Crack Detection	48
39. Eddy Current Bolt Hole Inspection dV / dt vs. t	49
40. Eddy Current Bolt Hole Inspection V_1 vs. V_2	50
41. Eddy Current Bolt Hole Inspection V_1 vs. V_2	51
42. Eddy Current Bolt Hole Inspection $\frac{dV_1}{dt}$ vs. $5 \frac{dV_2}{dt}$	53
43. Generalized Eddy Current Bridge	54
44. Electronics for Collection of Quantitative Eddy Current Data	57
45. Bridge Circuit for Calibrated Impedance Plane Data	58
46. Location in Impedance Plane of Eddy Current Coil Sensing Aluminum Brazing Material in Titanium Honeycomb Test Part	60
47. Passage of Eddy Current Coil Over Core Cell of Aluminum Brazed Titanium Honeycomb Panel	61
48. Effect of Change in Titanium Face Sheet Thickness	63
49. Heavy Aluminum Brazing vs. Light Aluminum Brazing	64
50. Equipment for Collection of Quantitative Eddy Current Data	65
51. Mutual Inductance Bridge for Calibrated Double Coil Eddy Current Data	66
52. Eddy Current Probe on Flat Iron Bar Being Subjected to D. C. Magnetization	68
53. Location of Ferrous and Nonferrous Metals in the Voltage Plane	69
54. Eddy Current Reaction to Three Types of Ferrous Flat Bar Being Subjected to D. C. Magnetization	71

INTRODUCTION

This is the final report covering a twelve month study for the Advanced Research Projects Agency on the application of electronic signal processing to nondestructive test measurements. The report period represents the second phase of an investigation in which modern signal detection and signal analysis techniques have been used to increase the sensitivity and reliability of NDT systems. During the first phase, analysis of statistical communication theory and available signal processing instruments led to several experiments involving ultrasonic and eddy current systems. Based upon the results of this initial eight month investigation, certain promising processing techniques were selected for more intensive study in the second phase. Attention has been given to both electronic and optical signal processing techniques.

The work during this phase has been in four principal areas: 1.) Signal averaging techniques have been used to detect ultrasonic flaw signals in the presence of coherent noise. In addition, a method of electrically tracking ultrasonic signals from weld discontinuities has been used to improve the clarity of flaw indications. 2.) As an aid to subsequent analysis and display of ultrasonic scan data, a procedure for using a low frequency tape recorder to record and play back ultrasonic video signals has been developed. 3.) Initial experiments have been performed in an evaluation of the use of optical processing techniques to carry out matched filtering and image enhancement of NDT data recorded in a two-dimensional, intensity modulated format. 4.) A lock-in amplifier has been used to obtain quantitative data in through transmission eddy current tests. Signal averaging and lock-in amplification have been used to produce quantitative data for single and double coil, single-side eddy current tests. Several practical applications of the above techniques have been investigated.

DISCUSSION

SIGNAL AVERAGING IN ULTRASONIC WELD INSPECTION

Theory

Present ultrasonic flaw detection systems are limited in sensitivity by background noise from a number of sources. Reflections of ultrasonic energy from non-flaw scattering centers within the test part and multipath sound transmission are two possible sources. In contrast to random signals, noise of this kind presents a stable display on a CRT for a fixed transducer position. In the present report all such signals, other than the flaw signal itself, will be referred to as "coherent noise". Random noise in ultrasonic systems usually results from the operation of amplifiers at high gain, and is most likely to be encountered in through-transmission tests involving highly attenuating media. Signal averaging effectively reduces random noise⁽¹⁾. The experiments of this section and the following three sections of the report are applications of signal processing to the reduction of coherent background noise.

Transducer ringing is one source of coherent noise. Flaws which are close to the front surface of a test part can easily be lost in such noise. The common solution to this problem is transducer damping. The use of pulse echo Lamb waves for surface flaw inspection can be limited by multiple internal reflections in the lucite wedge or other coupling medium employed. One solution is to employ a two transducer through transmission system. Even this system is limited by the receipt of sound waves passing directly between the two transducers rather than first reflecting off of a flaw. This coherent noise can be reduced by maintaining a ninety degree angle between the two transducers⁽¹⁾. In general, it is important to optimize the combination of transducer, pulser-receiver, cables, and transducer-test part geometry. Practical experience in this laboratory has indicated that the strength of ultrasonic flaw signals and the amount of background noise is strongly dependent on factors of this kind. Improvements such as those described above should be sought before applying electronic signal processing techniques to the problem.

Ultrasonic energy scattered by grain boundaries and inclusions within the test part cannot be effectively reduced by conventional procedures. In the present work, signal averaging has been used to improve the signal to coherent noise ratio of extended but very tight interface discontinuities in an electron beam welded panel. Weld discontinuities of this kind are produced by lateral displacement of the very narrow electron beam during welding and can be of marginal detectability using conventional gating techniques. Details are presented below.

Apparatus

A photograph of the equipment employed appears in Figure 1, and the transducer-test part geometry is shown in Figure 2. The inspection was performed using pulse-echo shear wave at 5 MHz. A Sperry UM721 was used as pulser receiver and signal gating was performed with the PAR Model 160 Boxcar Integrator. In addition to serving as a gate, the boxcar integrates or averages the signal for a time selectable by a front panel adjustment. Averaging times up to 100 seconds are available. The output of the boxcar gate was connected to the Y axis of a Moseley 7000A recorder. The X position of the recorder pen was synchronized to the transducer position through the use of a ten turn potentiometer which acted as an electro-mechanical transducer. A Tektronix 551 oscilloscope provided a simultaneous display of the boxcar gate position and the video signal from the reflectoscope. The transducer scanning motion and a block diagram of the electronics are shown in Figure 3.

Data and Conclusions

For the test specimens available, all known discontinuities were detectable using conventional pulse echo shear techniques, if repeated scans were made with careful attention being given to the lateral distance between the transducer and the weld line. However, a misalignment of three-tenths of an inch produced flaw signals which were not discernable from the coherent noise background. The data obtained is shown in the upper curve in Figure 4. Although the two flaws on the left are still clearly visible there are three more inch-long flaws in the specimen. It should be emphasized that if these were not tight interface flaws they would all be readily detectable. If the same ultrasonic information is gated by the boxcar integrator, and if one uses a constant scan rate and an appropriate averaging time, the lower curve of Figure 4 results. Each of the other three flaws can now be seen. The tight interface discontinuities are all one inch in length while the coherent background noise commonly varies considerably over a one-sixteenth inch transducer movement. Viewing the integration as a low pass filter, the lower frequency flaw information was retained while the higher frequency background noise was rejected. By inspecting various recorded scans the operator will notice that there is an optimum averaging time for a given scan rate.

ULTRASONIC WELD INSPECTION WITH A MOVING GATE

Theory

The signal to coherent noise ratio of the ultrasonic signal obtained from a tight interface discontinuity in an electron beam weld has been improved using a narrow electronic gate with an electrically controllable delay. The narrow gate cuts out much of the background noise that would be included in a wider gate.

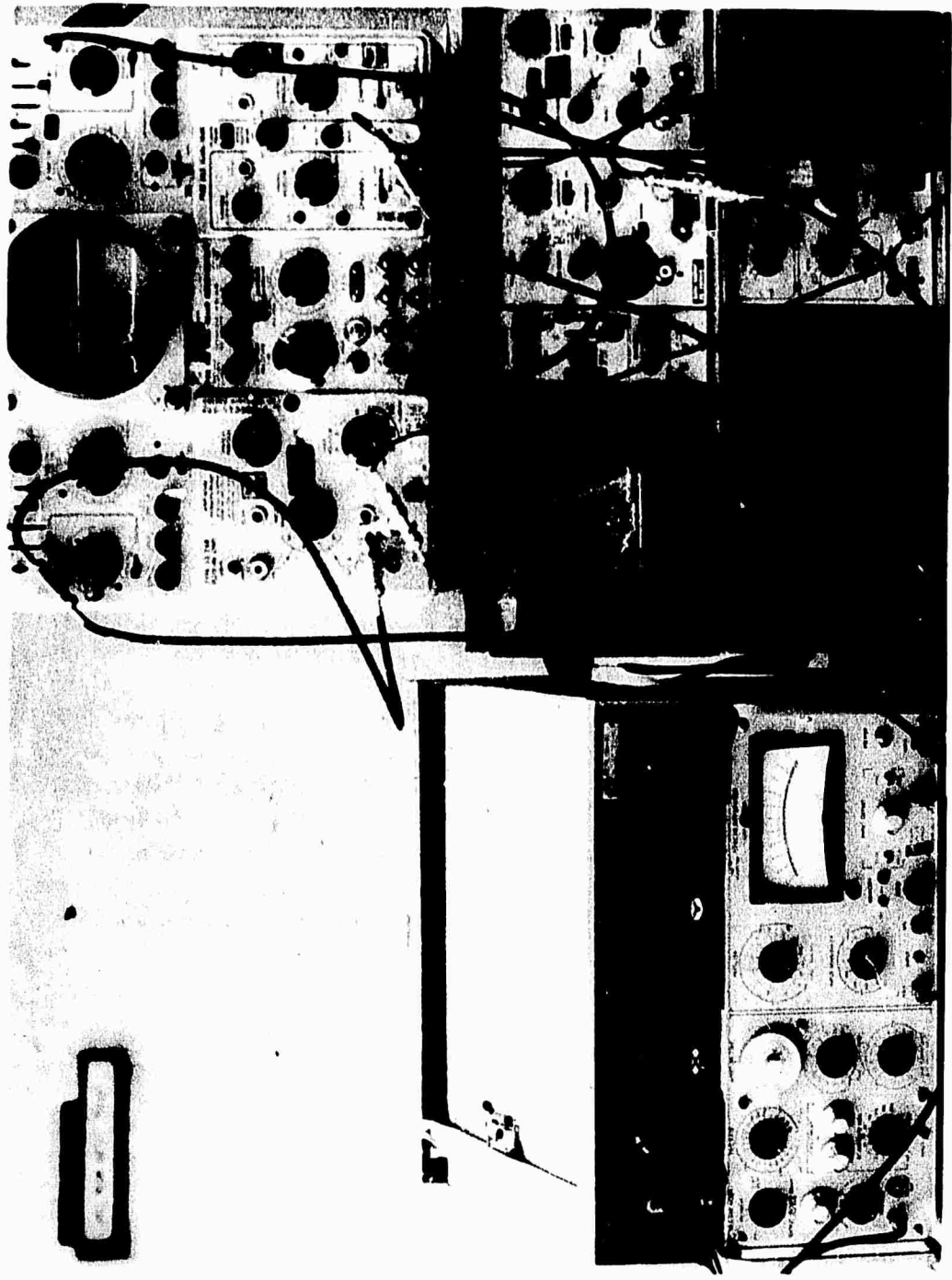


FIGURE 1 EQUIPMENT FOR SIGNAL AVERAGING IN ULTRASONIC WELD INSPECTION



FIGURE 2 TEST SPECIMEN AND TRANSDUCER FOR ULTRASONIC WELD INSPECTION

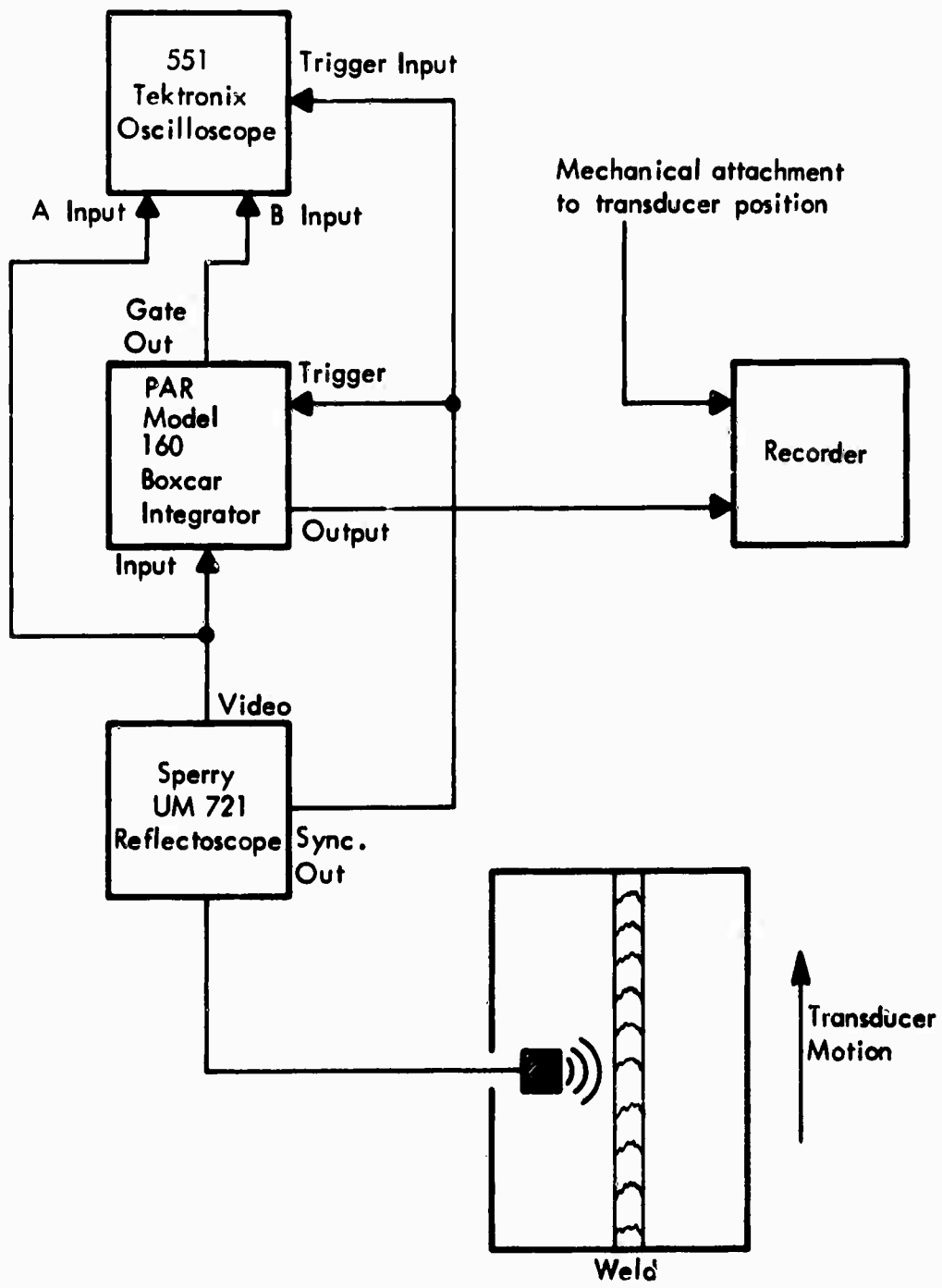


FIGURE 3 ELECTRONICS FOR SIGNAL AVERAGING IN ULTRASONIC WELD INSPECTION

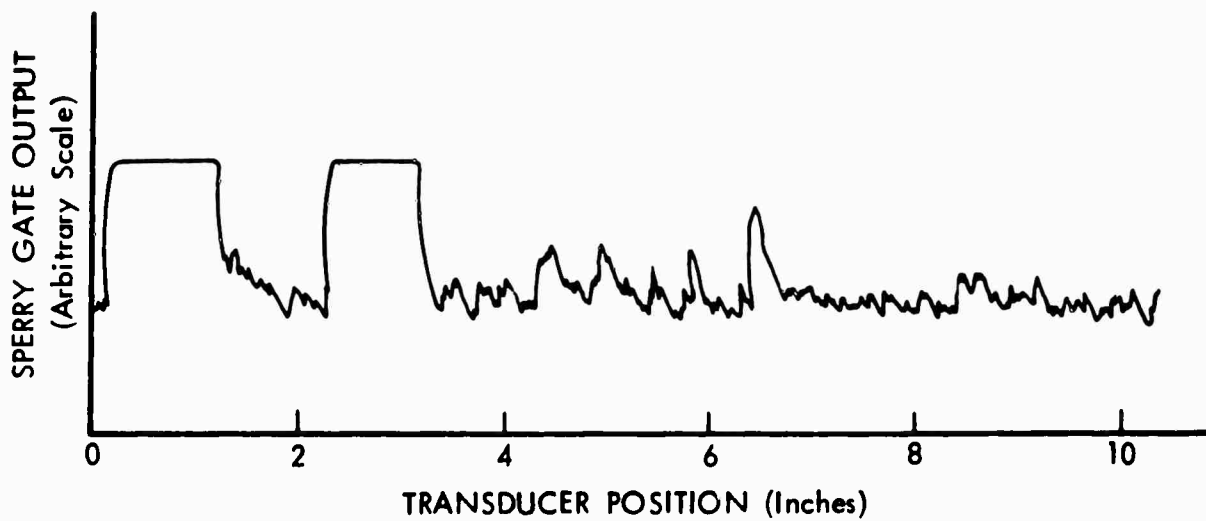


FIGURE 4 SIGNAL AVERAGING DATA

The electrically controllable delay insures that the narrow gate is properly placed for detection of ultrasonic reflections from the weld area by synchronizing the gate position with the transducer position.

During the C-scan inspection of a weld, the transducer continuously shuttles back and forth in a direction perpendicular to the length of the weld. Observation of the changing CRT display which results from this shuttle motion reveals an irregularly varying background noise and flaw signals which exhibit regular time delay and amplitude variations. The flaw signal time delay appears to be synchronized with the transducer position. By synchronizing the boxcar gate delay to the transducer position, the gate appears to follow the flaw signal as the transducer shuttles. This synchronization can be accomplished by sensing the location of the ultrasonic probe with a position transducer and feeding the resulting signal into the gate delay input jack of the boxcar integrator. A choice of averaging times is also available in this mode of operation.

Apparatus

A block diagram of the equipment appears in Figure 5. With the exception of the use of the gate delay input, the equipment is similar to that described in the previous section. The position potentiometer is mechanically attached to the transducer holder. A small rubber tire is fastened to its shaft. As the ultrasonic transducer moves, the tire rolls along the edge of the inspection tank. The resulting resistance change is converted into a DC signal and connected to the gate delay as shown in Figure 5.

Data and Conclusions

The test part was an electron beam welded titanium tensile specimen. There are no artificial flaws in the specimen and the indication being studied appears to be due to a real discontinuity. Data for one shuttle pass, presented in A-scan form, appears in Figure 6. Data was initially collected by conventional means selecting a gate width encompassing the full depth of the weld. The result obtained using the standard gate within the Sperry UM721 ultrasonic instrument appears in the upper curve. Data collected using the boxcar moving gate with signal averaging appears in the lower curve. A significant reduction in background coherent noise can be seen.

TAPE RECORDED ULTRASONIC INFORMATION

Theory

The Model 160 Boxcar Integrator has been used to produce tape recordings of pulse echo ultrasonic inspection information. The ultrasonic information was recorded by causing the boxcar gate to sweep at 50 Hz through a time interval corresponding to the thickness of the test object, thus producing a low frequency

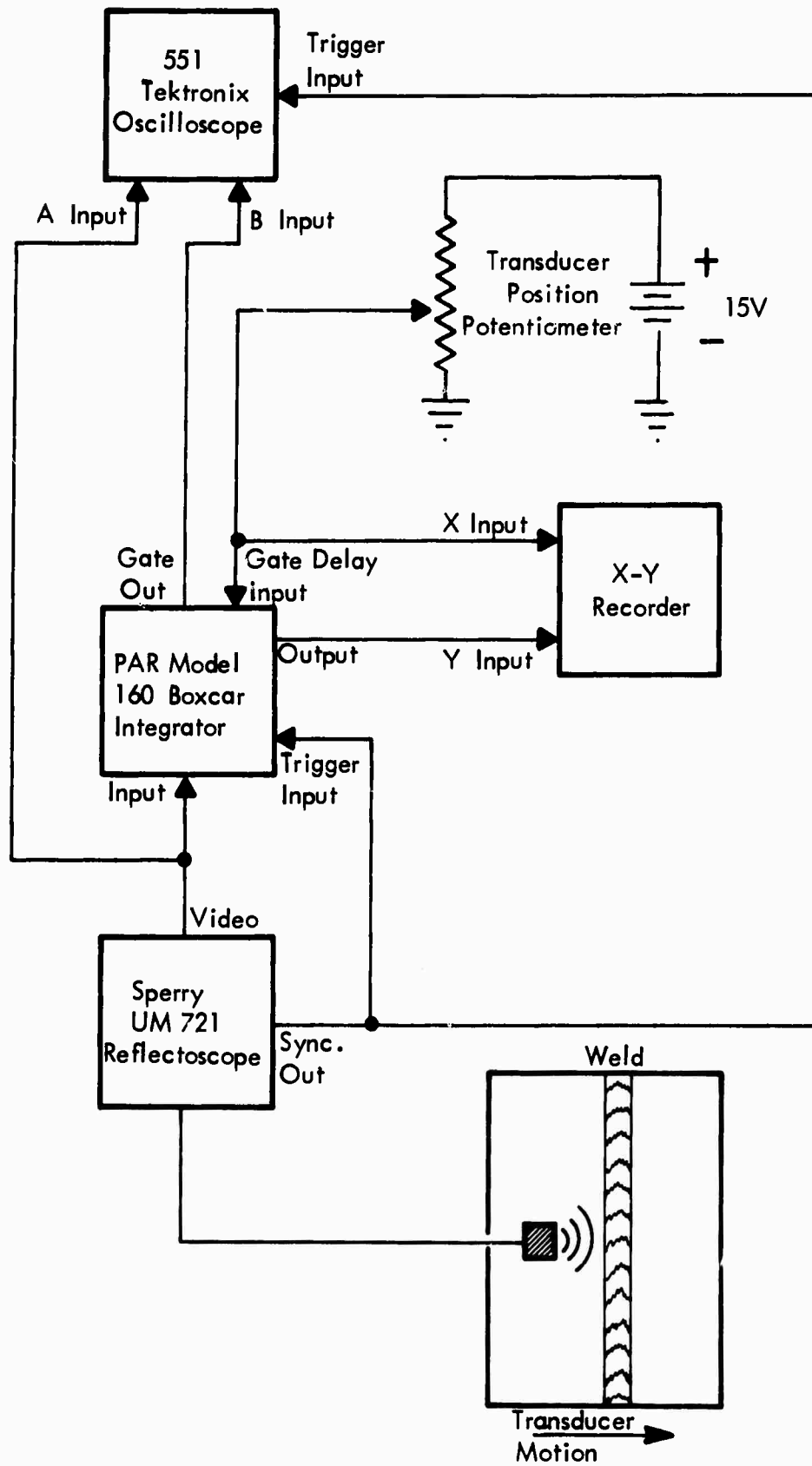


FIGURE 5 ELECTRONICS FOR WELD INSPECTION WITH A MOVING GATE

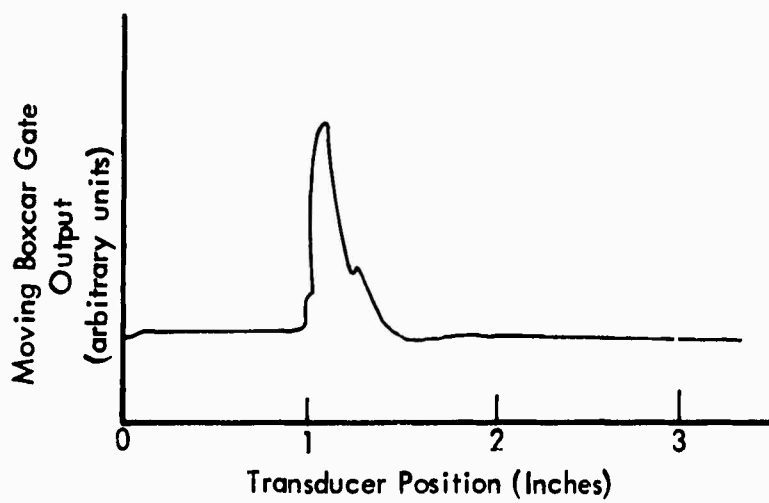
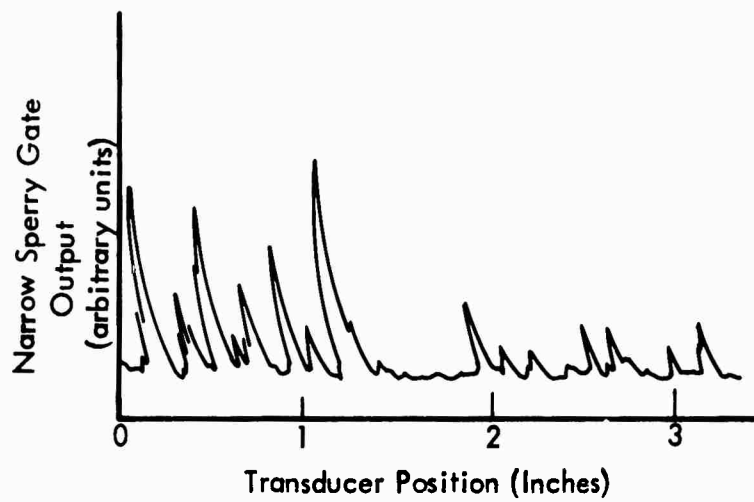


FIGURE 6 MOVING GATE DATA

replica of the video signal. A direct-FM recorder employing magnetic tape with a maximum frequency response of 50 KHz was used. Information from all regions of the test specimen is collected and no information is lost as a result of conventional time gating before tape recording. Various regions of interest at selectable depths within the part may be rapidly examined through conventional gating during playback of the tape recordings. The tape can be played back at an increased rate of speed so that various ultrasonic signal processing techniques can be quickly evaluated.

An interesting operation that can be performed on playback is the production of a C-scan display on a storage oscilloscope. One can quickly produce a C-scan image of any reflecting plane perpendicular to the ultrasonic beam and can readily evaluate the effects of various triggering levels. Several typical C-scan images appear in the data section.

Apparatus

Figure 7 is a photograph of the equipment used and Figure 8 is a block diagram of the electronics when the system is in the record mode. The Sperry UM721 was operated in the pulse-echo mode. Longitudinal waves were excited in the test block and a raster transducer scan technique was used to examine all portions of the test object. The Tektronix 551 allowed simultaneous viewing of the video signal from the Sperry Reflectoscope and the position of the boxcar gate. The Tektronix 515A was used to supply the sawtooth signal which causes the boxcar gate to sweep through the time interval of interest at 50 Hz. Since it is necessary that the sawtooth be synchronized with the kilocycle repetition rate of the reflectoscope, the 515A was triggered by the Sperry sync signal. It is somewhat difficult to synchronize a 50 Hz signal with a 1 KHz signal and the 515A performed the task better than any other device at our disposal. The sweeping of the gate at 50 Hz was accomplished by connecting the sawtooth signal to the gate delay input of the boxcar integrator. The time interval over which the boxcar gate was sweeping was readily visible on the screen of the Tektronix 551. This permitted adjustment of the time delay to insure that the gate swept through that portion of the video signal which was to be recorded. The start point of the range was determined by the D.C. power supply and the length of the range was determined by the amplitude of the sawtooth signal. A low frequency replica of the desired portion of the video signal appeared at the boxcar output. For the frequencies under consideration, the signal at the boxcar output was actually a twenty (1000 Hz/50 Hz) point sample of the desired video signal. A sample of this size was found to be adequate for the inspection of a one inch thick aluminum block. If the signal is passed through a smoothing filter, it looks very much like the actual video. If a larger sample seems necessary, the sweep rate must be slower and the ultrasonic scanning rate will have to be reduced until the video signal does not change significantly over one sawtooth period.

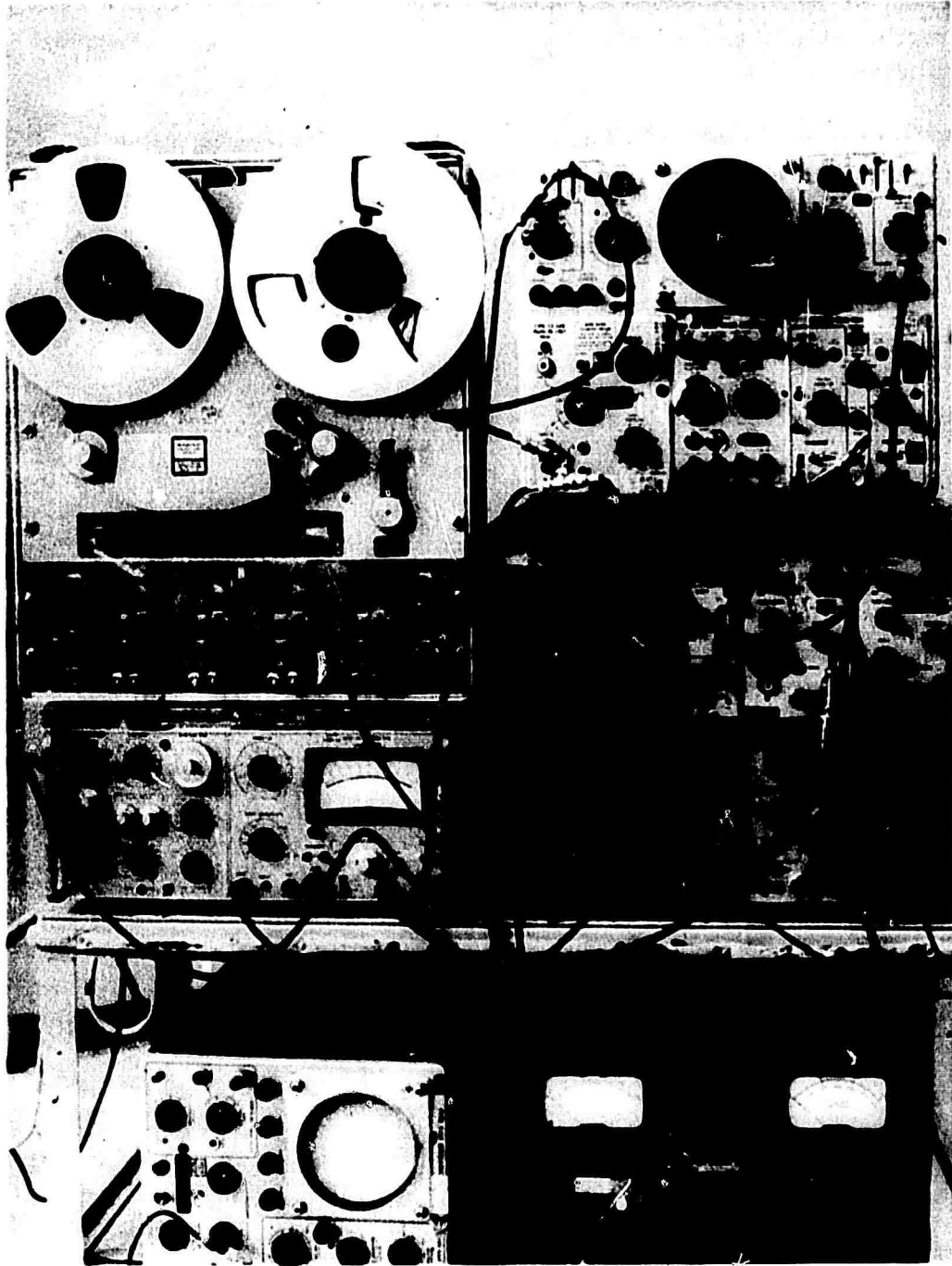


FIGURE 7 EQUIPMENT FOR TAPE RECORDING ULTRASONIC INFORMATION

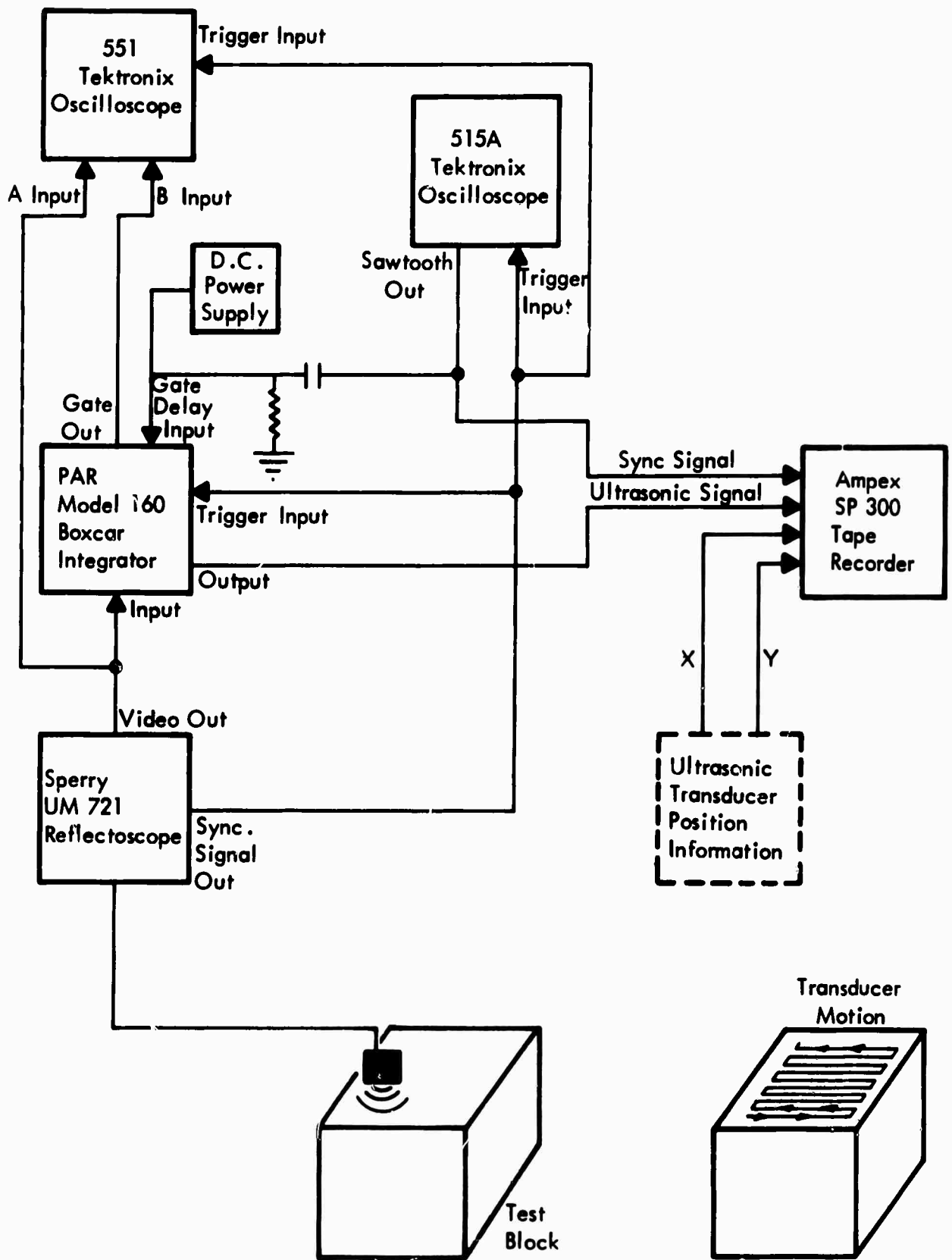


FIGURE 8 ELECTRONICS FOR TAPE RECORDED ULTRASOUND-RECORD MODE

The low frequency replica of the video signal was connected to the input of an Ampex SP300 tape recorder. This is a direct/FM recorder with a maximum frequency response of 50 KHz. The sawtooth, or a related signal, should be simultaneously recorded to provide a sync signal to be used on playback. If desired, it is also possible to record the position of the ultrasonic probe. Two D.C. voltages corresponding to the X and Y location of the ultrasonic probe can be obtained through the use of position transducers. Four-channel recording capability for the SP300 is readily available.

In the present work the ultrasonic information was removed from the tape and presented as a C-scan display on a storage oscilloscope. The block diagram of the electronics for the playback mode appears in Figure 9. The SP300 operating in the playback mode acts as the source for all signals. The video is fed to the boxcar integrator just as it would be if it came from the Sperry reflectoscope. The sync signal, after amplification and smoothing, triggers the boxcar integrator and the oscilloscope. The Tektronix 516A allows simultaneous viewing of the low frequency "video" and the position of the boxcar gate. At this point the boxcar performs conventional gating. The gate delay and width are manually adjustable. As is normally the case, different gate positions correspond to different depths in the part. By viewing the CRT of the 516A and adjusting the boxcar gate delay, the operator selects that portion of the part which he wishes to see. The gated "video" information is applied to the intensity modulation input of a storage oscilloscope. The position of the spot on the storage oscilloscope screen is determined by the ultrasonic probe location voltages, which are also coming from the tape recorder. The result is the production of a C-scan presentation of the ultrasonic energy reflected from the plane of interest within the test part. Use of the boxcar D.C. offset in combination with a fixed threshold voltage in the storage oscilloscope allows the operator to select any desired C-scan trigger level. Since the tape recorder is being played back at a higher rate of speed than was used for recording, the picture reproduction time is only 90 seconds. It should be possible to considerably reduce this time with a proper combination of equipment. With short picture reproduction times it will be possible for the inspector to search through the part, viewing different reflecting planes and different triggering levels in quick succession. Since a fairly narrow boxcar gate can be used the flaw sensitivity is higher than would be obtained if a conventional C-scan recording were made using a gate width corresponding to the entire thickness of the part.

Data and Conclusions

The test part was an aluminum block 2 in. by 2 in. by 1 in. A cross sectional diagram appears in Figure 10. It contains three #60 drill holes as shown. Figure 11 is the C-scan presentation of the ultrasound reflected from the front surface of the block. The horizontal axis is considerably amplified in this picture and the entire front surface of the block is not shown. This photograph corresponds

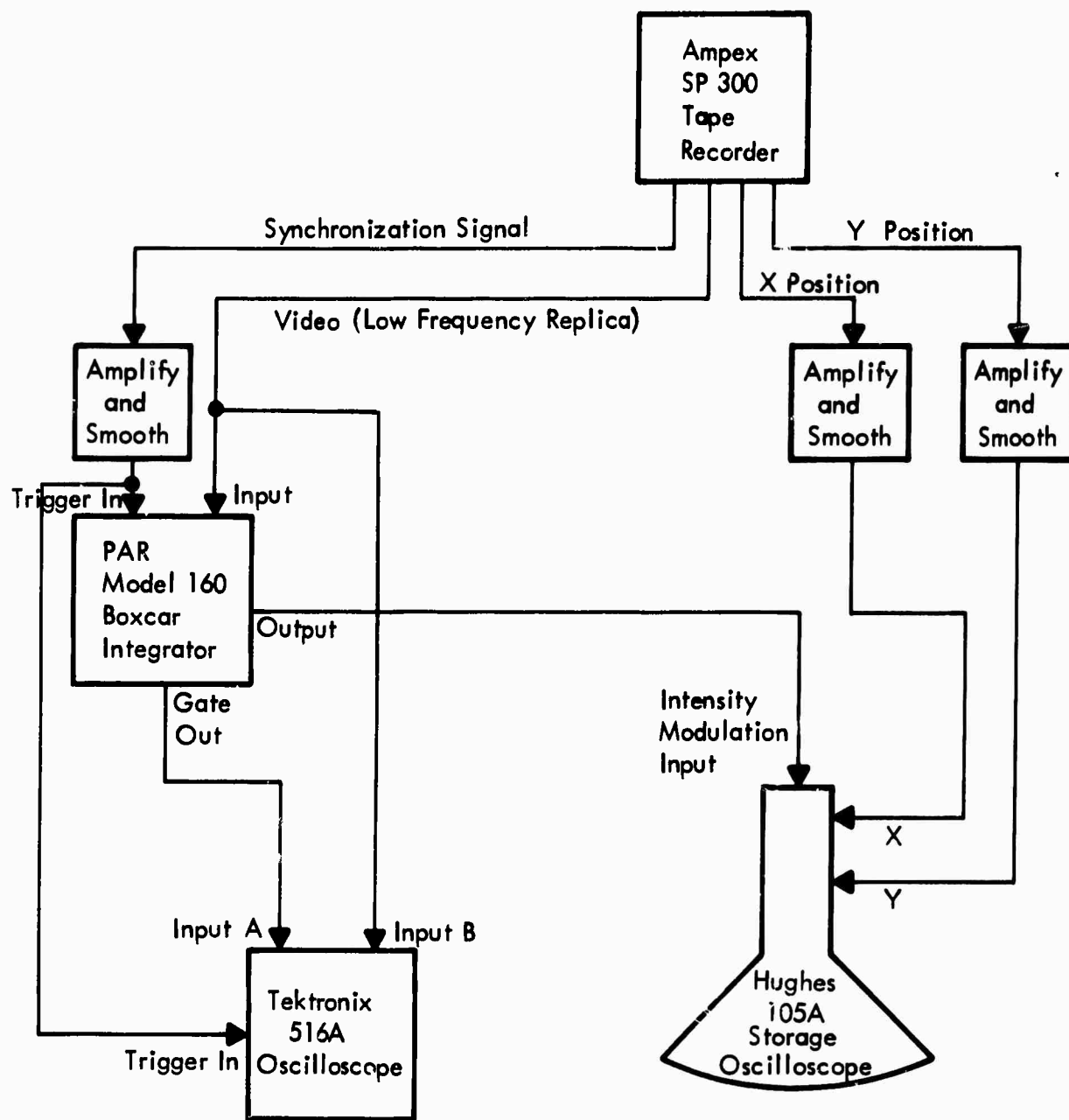


FIGURE 9 ELECTRONICS FOR TAPE RECORDED ULTRASOUND-PLAYBACK MODE

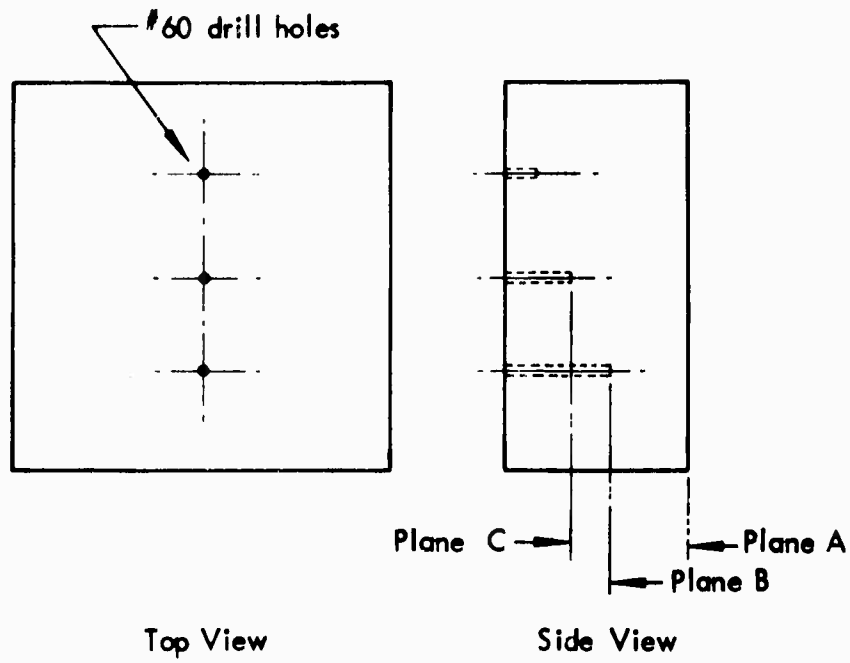


FIGURE 10 TEST PART USED FOR TAPE RECORDING ULTRASONIC FLAW INDICATIONS

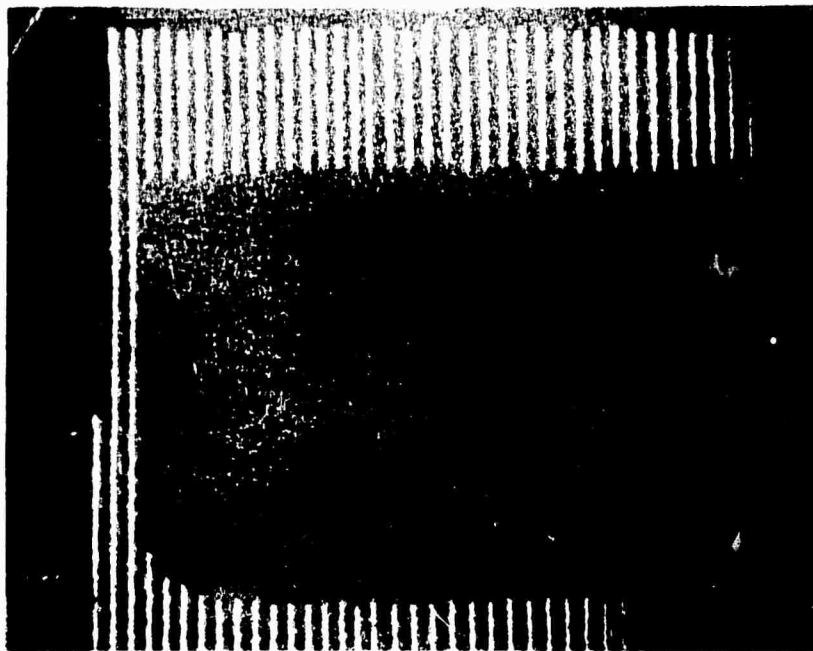


FIGURE 11 STORAGE OSCILLOSCOPE DISPLAY OF TAPE RECORDED ULTRASONIC INFORMATION

to a 25 line per inch ultrasonic scan. The outline of the block was traced on the front surface of the CRT with a grease pencil and appears in the photographs to follow. The top photograph of Figure 12 is a C-scan presentation of the ultrasonic energy reflected from plane B which coincides with the top of the deepest drill hole. The bottom photograph represents sound reflected from plane C. Notice that the drill holes are readily visible.

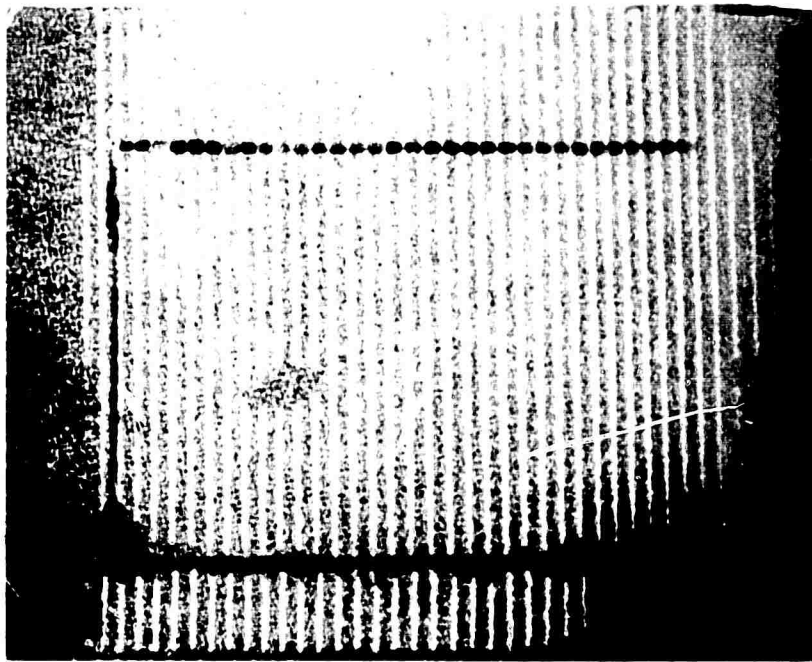
FILM RECORDED ULTRASONIC INFORMATION AND OPTICAL SIGNAL PROCESSING

Theory

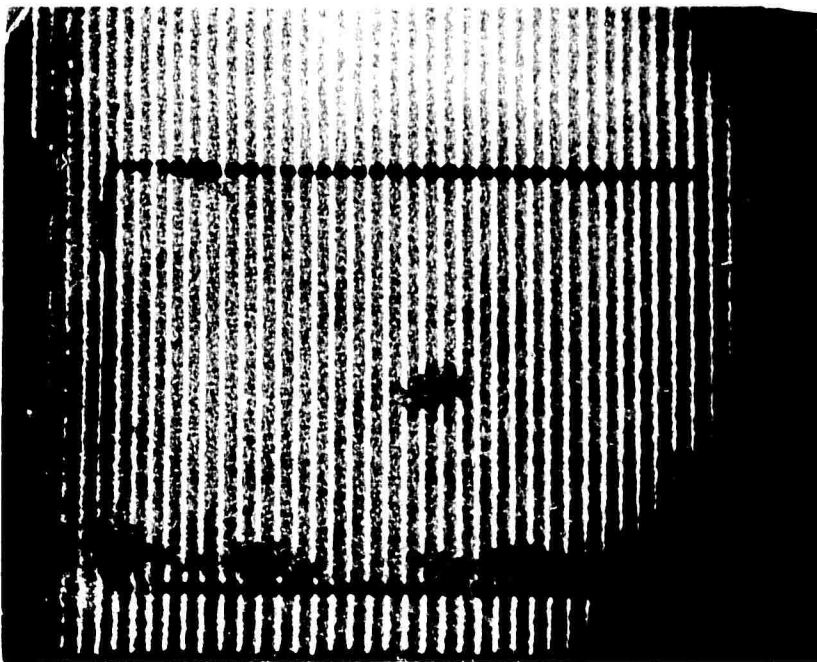
Ultrasonic C-scan information has been recorded on a photographic transparency. This recording was made in an effort to transform the ultrasonic information into a form susceptible to optical signal processing and is part of a general program to enhance flaw signals, and reduce coherent background noise by optical techniques. Pen and ink recordings of ultrasonic information obtained from a photographic transparency by a scanning densitometer indicate that high quality photographic recording and reproduction of ultrasonic information are possible.

The general signal processing program is outlined in Figure 13. The conventional way to perform a thorough ultrasonic inspection is to use C-scan methods, presenting the results in the form of a hard copy recording corresponding to the area inspected. Such recordings generally indicate by the presence or absence of a mark whether or not the ultrasonic signal has exceeded a predetermined trigger level. They do not contain all of the ultrasonic intensity information available. In the present work ultrasonic information has been recorded on a photographic transparency. This is accomplished by using the gated video signal to modulate the intensity of the electron beam in a CRT. The ultrasonic information appears at the face of the screen as brightness variations in a fine spot. The spot moves across the face of the CRT in synchronism with the C-scan motion of the ultrasonic probe. A time exposure is made using a Tektronix polaroid camera attachment. The result is a recording of all the information available, including all intensity levels. Future work will involve performing optical band pass filtering and optical matched filtering on this transparency. Both coherent and incoherent optical processing techniques will be investigated. Experiments with matched filtering using Vander Lugt techniques are planned. Opportunities exist for "coding" of the ultrasonic signal through the use of multiple transducers. As Figure 13 indicates, the ultrasonic information is removed from the film after processing. Use of an X-Y scanning densitometer allows the production of hard copy pen and ink recordings. The display of processed flaw indications by projection will also be considered.

The use of optical processing is particularly appropriate for the present problem because C-scan techniques produce ultrasonic information in a 2 dimensional format. Electrical low pass filtering has been considered and the results are



PLANE B



PLANE C

FIGURE 12 STORAGE OSCILLOSCOPE DISPLAY OF TAPE RECORDED
ULTRASONIC FLAW INDICATIONS

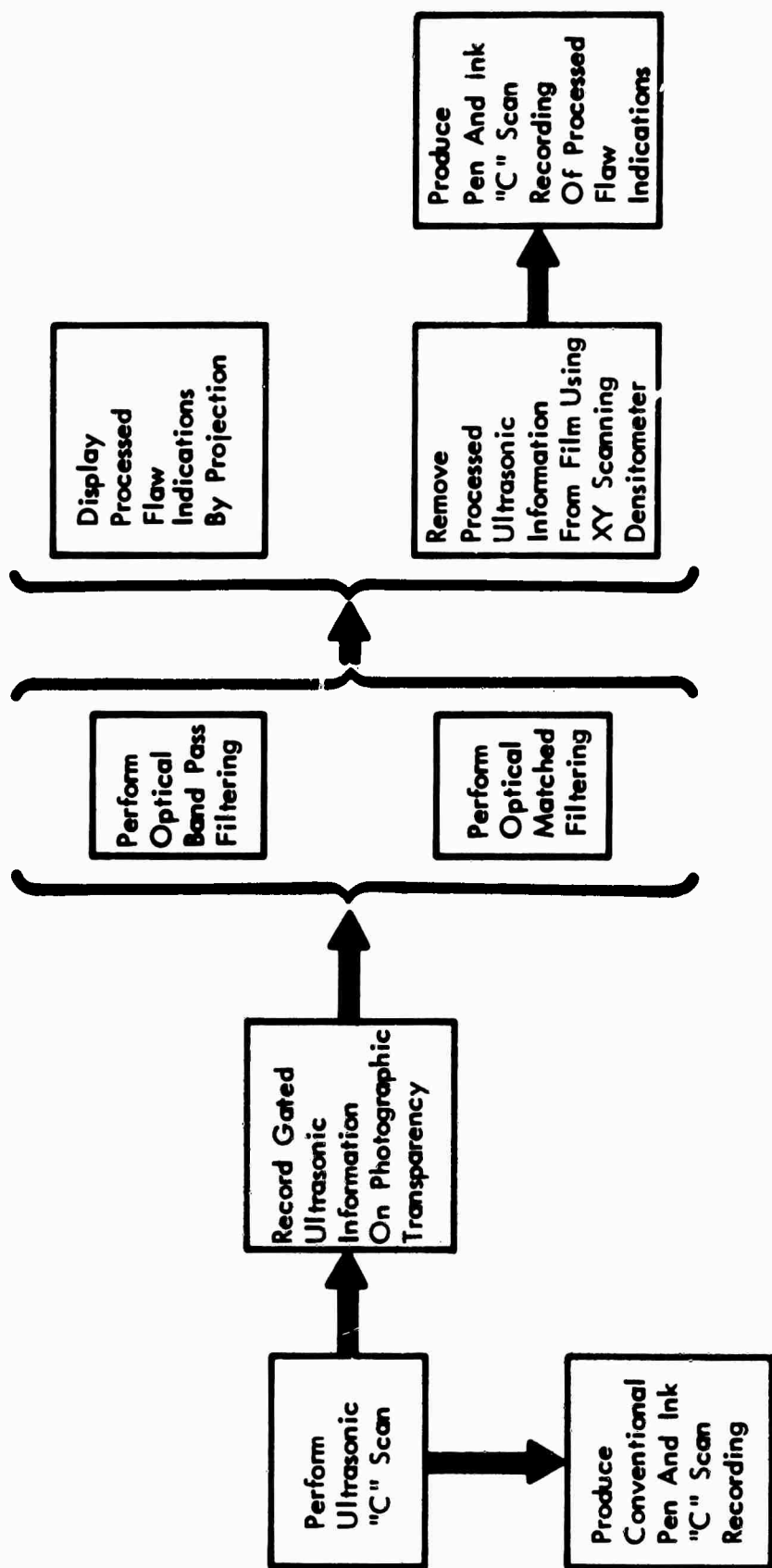


FIGURE 13 OPTICAL PROCESSING OF ULTRASONIC INFORMATION

presented in the section on signal averaging in ultrasonic weld inspection. It has been decided that electrical matched filtering would be considerably more difficult than optical matched filtering. A wide variety of coherent noise backgrounds and flaw signals is anticipated in actual practice. It is unlikely that electrical matched filtering could provide the flexibility required. The concept of matched filtering is attractive because it represents the optimal way of separating a signal from background noise.

Apparatus

Figure 14 is a block diagram of the film recording system and Figure 15 is a photograph of the equipment used. A UM721 reflectoscope was used as pulser-receiver and the gating was performed with the boxcar integrator. The oscilloscope provided a simultaneous display of the ultrasonic video signal and the boxcar gate position. The intensity modulation was accomplished with a 561A Tektronix oscilloscope. It was found that a type 3B4 time base unit produced the smallest spot on the face of the CRT. A small spot is necessary in order to obtain the desired information density. In the present work the ultrasonic scan was performed at 50 lines per inch, and the photographic transparency contained 50 lines per inch. The horizontal spot position was controlled by the time base unit operating in the external delayed trigger mode. The vertical position was determined by the output of a position transducer which was mounted on the ultrasonic probe holder.

Figure 16 is a photograph of the film readout system. It is an X-Y scanning densitometer constructed from a Moseley Autograf recorder. The densitometer can be operated in conjunction with an X-Y recorder to produce hard copy recordings in either A-scan or C-scan form.

Data and Conclusions

The test specimen was the same aluminum block used to collect data for the tape recording of ultrasonic information. A diagram appears in Figure 10. The parameters which affect system calibration are film type, camera aperture width, scan rate, oscilloscope intensity setting, and the amplitude and D.C. level of the gated video information. These factors can all be taken into account by the preparation of a calibration curve such as the one appearing in Figure 17. Each horizontal line corresponds to a different value of intensity modulation voltage. By visual inspection, or better, by use of the scanning densitometer a voltage range can be selected over which a linear film response is obtained.

A positive print of film recorded ultrasonic information obtained from the inspection of the aluminum block appears in Figure 18. The boxcar gate width used during the inspection corresponded to the full depth of the test block. Notice that two of the three flaws are visible as well as the outline of the test block. This mode of data presentation differs from conventional C-scan recordings in that all intensity information is present.

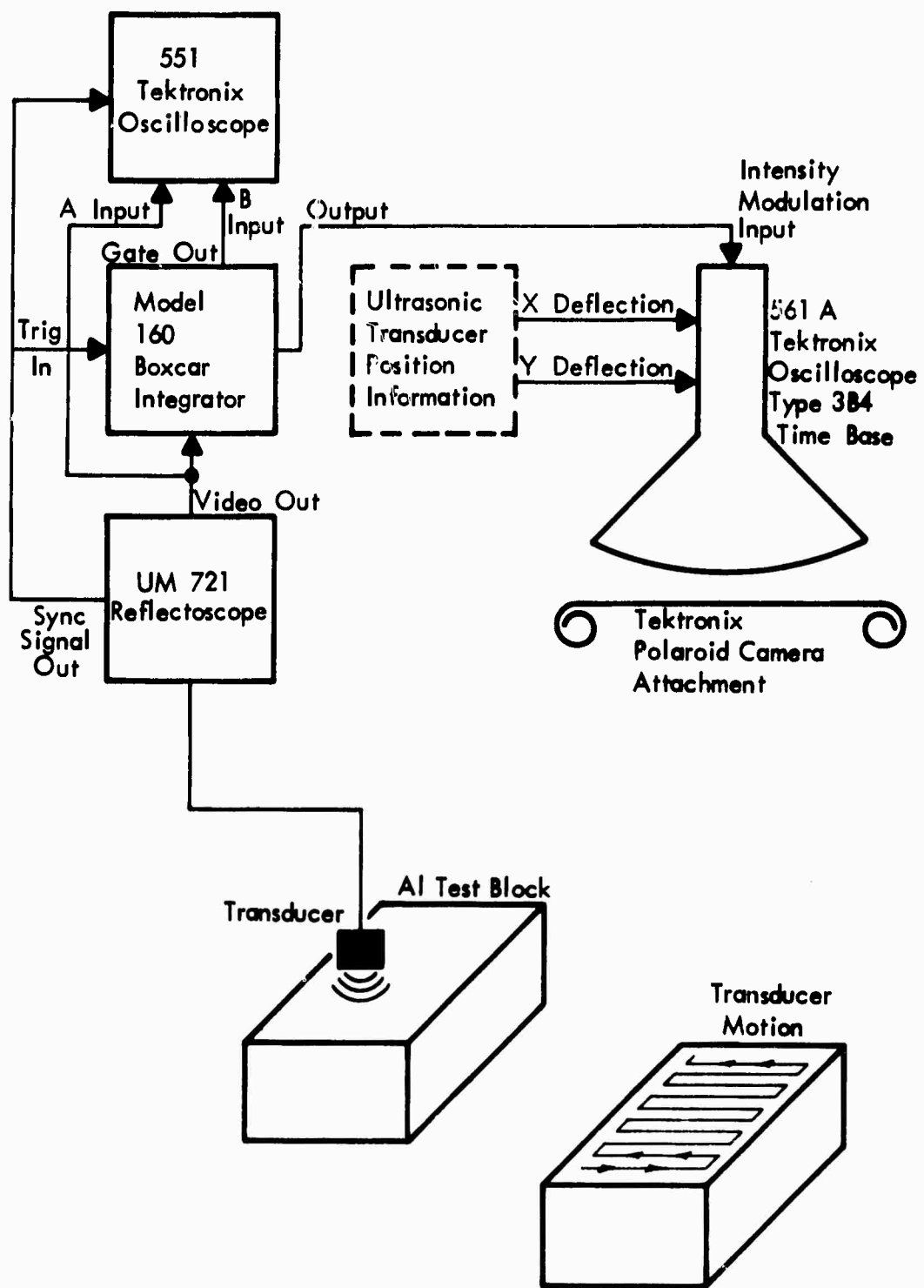


FIGURE 14 ELECTRONICS FOR FILM RECORDING ULTRASONIC INFORMATION

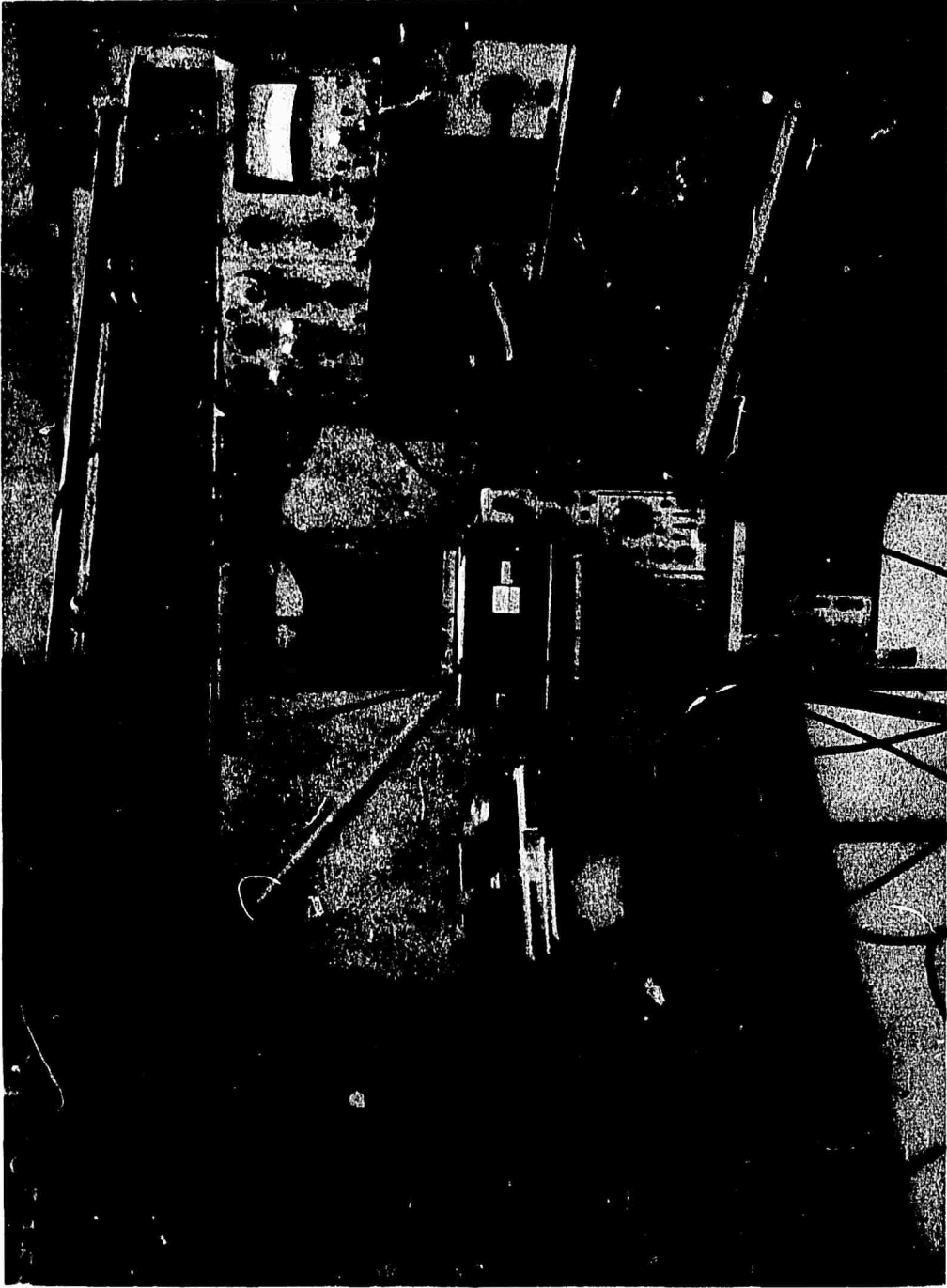


FIGURE 15 EQUIPMENT FOR FILM RECORDING ULTRASONIC INFORMATION

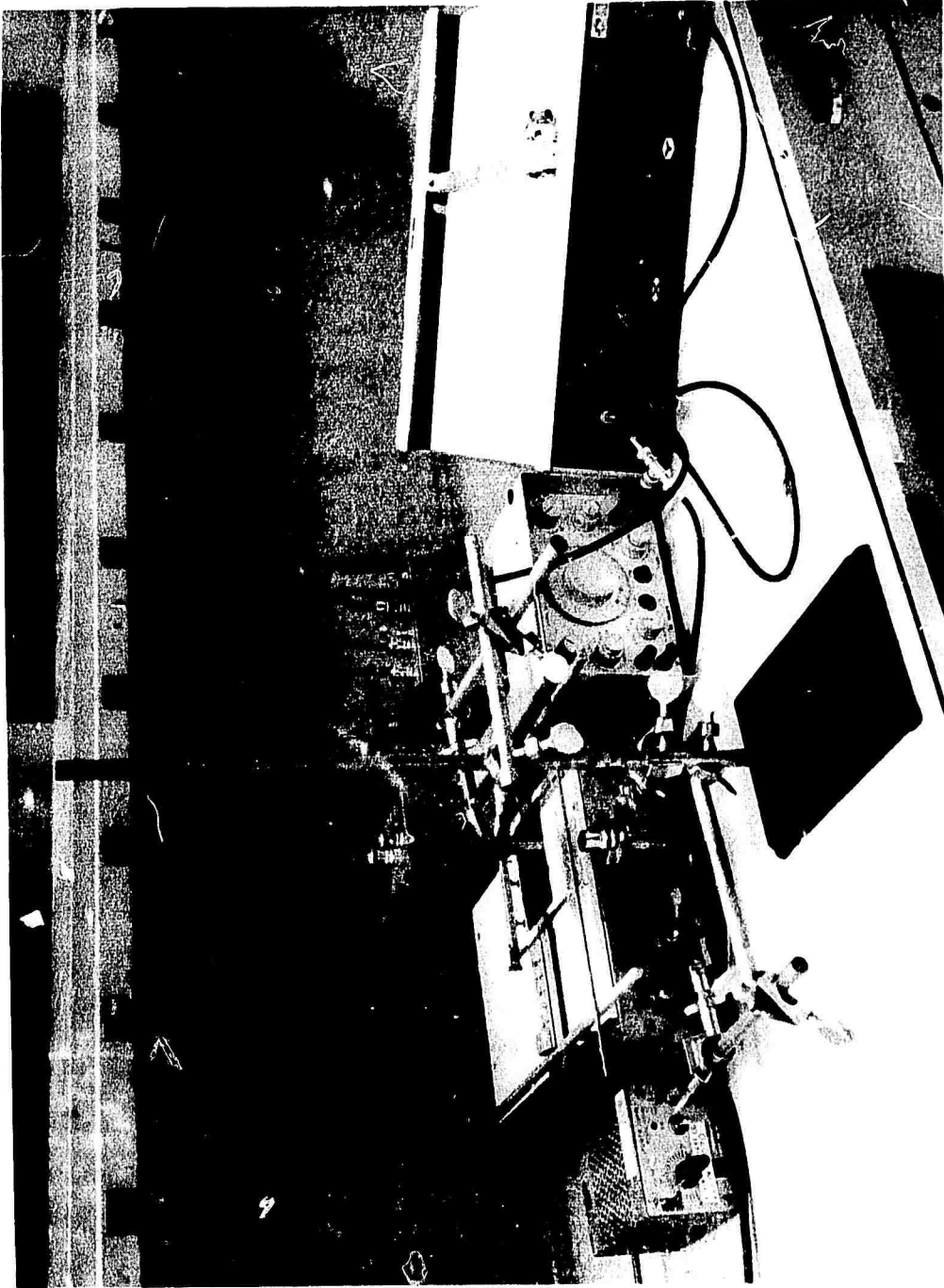


FIGURE 16 X-Y SCANNING DENSITOMETER



**FIGURE 17 CALIBRATION CURVE FOR FILM RECORDING
ULTRASONIC INFORMATION**



FIGURE 18 FILM RECORDED ULTRASONIC FLAW INDICATIONS

A conventional ultrasonic A-scan, taken along the centerline of the test block, appears in Figure 19. The first three peaks are the drill holes and the fourth peak is caused by an edge reflection. A similar curve produced with the densitometer by scanning across the centerline of the film appears in Figure 20. The high frequency oscillations correspond to individual scan lines and the envelope is the desired ultrasonic information. It is clear that there is much more information on the photographic transparency than appears in Figure 18. The lower portion of the flaw indications appears cut off because the region of linear film response was accidentally exceeded. These recordings indicate that high quality film recording and reproduction are possible. Knowing that the ultrasonic information is accurately recorded on the transparency, one can confidently proceed with the optical signal processing.

EDDY CURRENT THROUGH TRANSMISSION TESTING

Theory

A commercial lock-in amplifier has been used to perform through transmission eddy current testing. The use of a lock-in amplifier in combination with a power amplifier and two eddy current coils has proven to be a convenient way to produce quantitative through transmission eddy current data. The availability of quantitative data has aided in the design of test equipment and has been of value in the establishment of optimum operating conditions.

A through transmission eddy current system employs two test coils. One acts as a transmitter and the other as receiver. The test part is placed between the coils. If the transmit coil carries a sinusoidal driving current, and if the test part is absent, a voltage $V_o \cos(\omega t)$ is induced in the pickup coil. If a metallic specimen is placed between the coils, the electromagnetic wave propagating from transmitter to receiver experiences attenuation and time delay. The voltage induced in the pickup coil is attenuated to V' and phase shifted by an amount ϕ . With the test part in place the voltage across the pickup coil can be written,

$$V'_o \cos(\omega t - \phi) = V_{in} \cos(\omega t) + V_{quad} \cos(\omega t - \pi/2)$$

where,

$$V_{in} = V'_o \cos \phi \quad \text{and} \quad V_{quad} = V'_o \sin \phi$$

Using a lock-in amplifier one can make independent measurements of V_{in} and V_{quad} as a function of frequency. All of the eddy current information available is contained in V' and ϕ . Note that none of the information is lost by measuring V_{in} and V_{quad} because one can write,

$$V'_o = \sqrt{V_{in}^2 + V_{quad}^2} \quad \text{and} \quad \tan \phi = \frac{V_{quad}}{V_{in}}$$

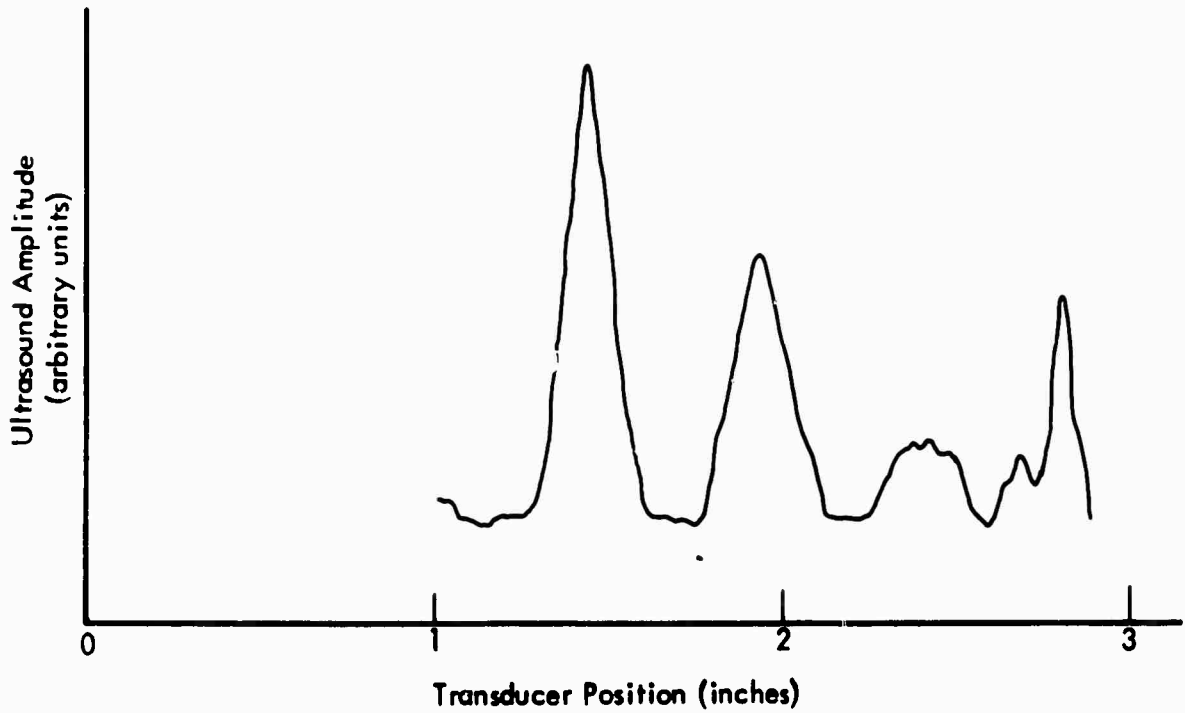


FIGURE 19 CONVENTIONAL "A" SCAN RECORDING OF ULTRASONIC FLAW INDICATIONS

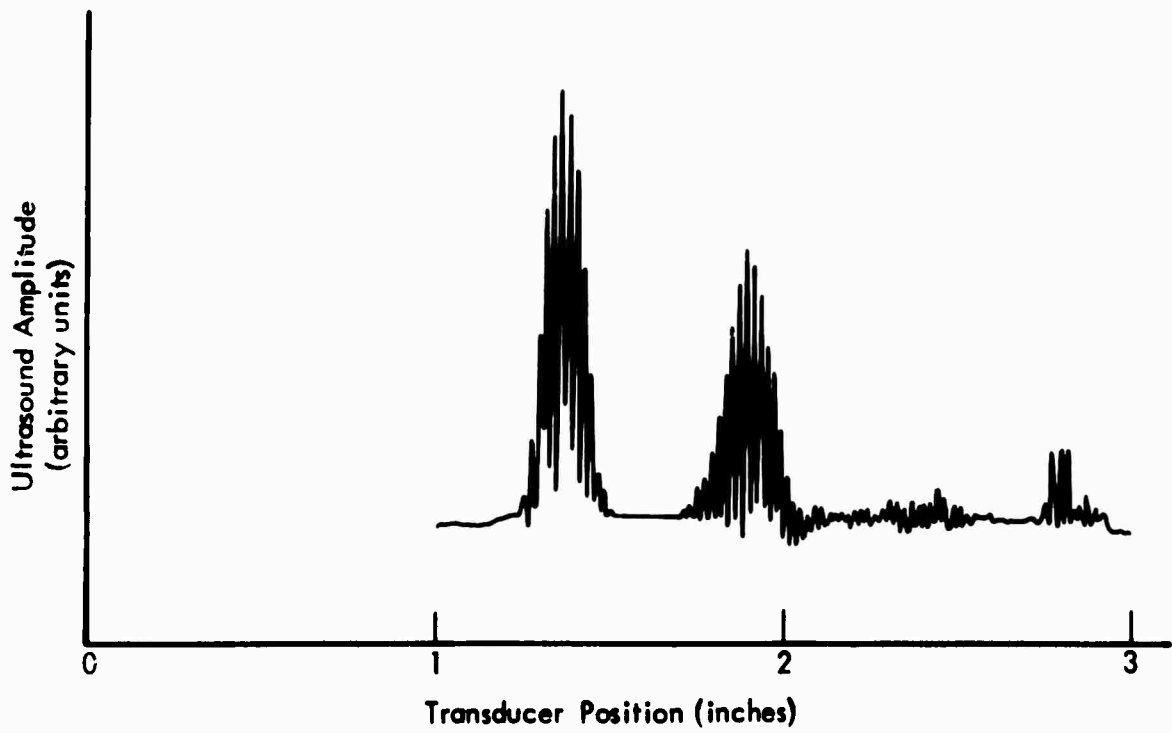


FIGURE 20 "A" SCAN PRODUCED FROM FILM RECORDED FLAW INDICATIONS

Apparatus

Figure 21 is a circuit diagram of the through transmission eddy current system used in the present work. A Princeton Applied Research HR-8 lock-in amplifier serves both as signal generator and signal detector. The HR-8 is an averaging instrument capable of separating cw signals from random noise backgrounds. Except for particularly thick specimens, random noise is not a problem in this type of work and the HR-8 is being used because it is also a phase sensitive detector. The instrument is continuously tunable from 1.5 Hz to 150 KHz. Over that range it performs the functions of an oscillator, preamplifier, tuned amplifier, and phase sensitive detector. Measurements can be made down to the nanovolt range. A power amplifier feeds the transmit coil with approximately 1/2 ampere in order to obtain a strong signal at the pickup coil. A resistor in the transmit line minimizes phase shift in the transmit current when the test part is put in place. A resistor in the receive line serves as an impedance match with the HR-8 preamplifier. The transmit and receive coils consist of several hundred turns of copper wire wound on ferrite cores. They are approximately one half inch in diameter, and are mounted face to face approximately one half inch apart. Sheet material, held in a vertical plane, is placed between the coils for measurements.

Data and Conclusions

Through transmission eddy current data was collected on a sample of 6061-T4 aluminum 24 inches on a side and 0.063 inch thick. Measurements were made from 20 Hz to 130 KHz. At each frequency, the pickup voltage V_o was measured with the test part removed from the coils. The test part was then placed between the coils and measurements were made of the voltages in phase V_{in} and in quadrature V_{quad} with V_o . The ratios V_{in}/V_o and V_{quad}/V_o were calculated and a plot of the results appears in Figure 22. The curve does not pass directly through the origin as has been commonly reported (2) but passes around it forming a spiral of rapidly decreasing radius. The decreasing radius corresponds to the increase in attenuation with frequency. The fact that the curve passes through all four quadrants reveals phase shifts in excess of 360 degrees. To obtain very accurate data the investigator should take into consideration the phase shift of the current in the transmit coil due to the presence of the part and the phase shifts between the various gain levels in the lock in amplifier. In the present work corrections were made for phase shifts as small as 0.1 degree. Maximum current shifts were 0.6 degree. Phase shifts between the various gain levels of the HR-8 did not exceed 2.5 degrees. Such values indicate that approximate data, accurate enough for most practical purposes, can be collected in a fairly short time by ignoring these factors. In Figure 23 the through transmission eddy current data is replotted to exhibit the oscillatory frequency dependence of V_{in} and V_{quad} .

Through transmission eddy current data was collected on a set of 6061-T4 aluminum samples with thicknesses of 19.8, 40.8, 63.8, 78.9, 99.5 and 160.8 mils. Each sheet was 24 inches on a side. In order to exhibit the quality of data obtainable

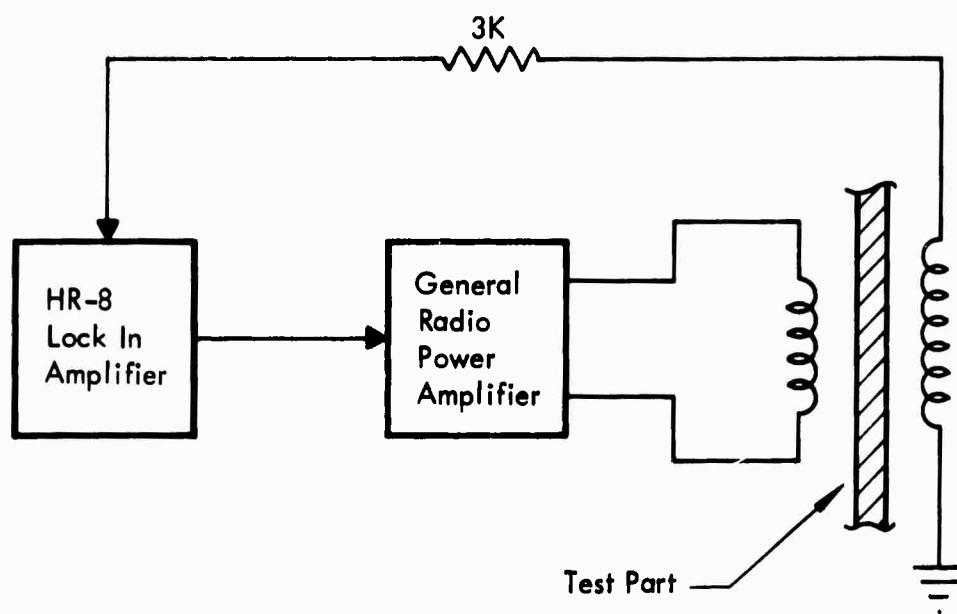


FIGURE 21 CIRCUITRY FOR THROUGH TRANSMISSION
EDDY CURRENT TESTING

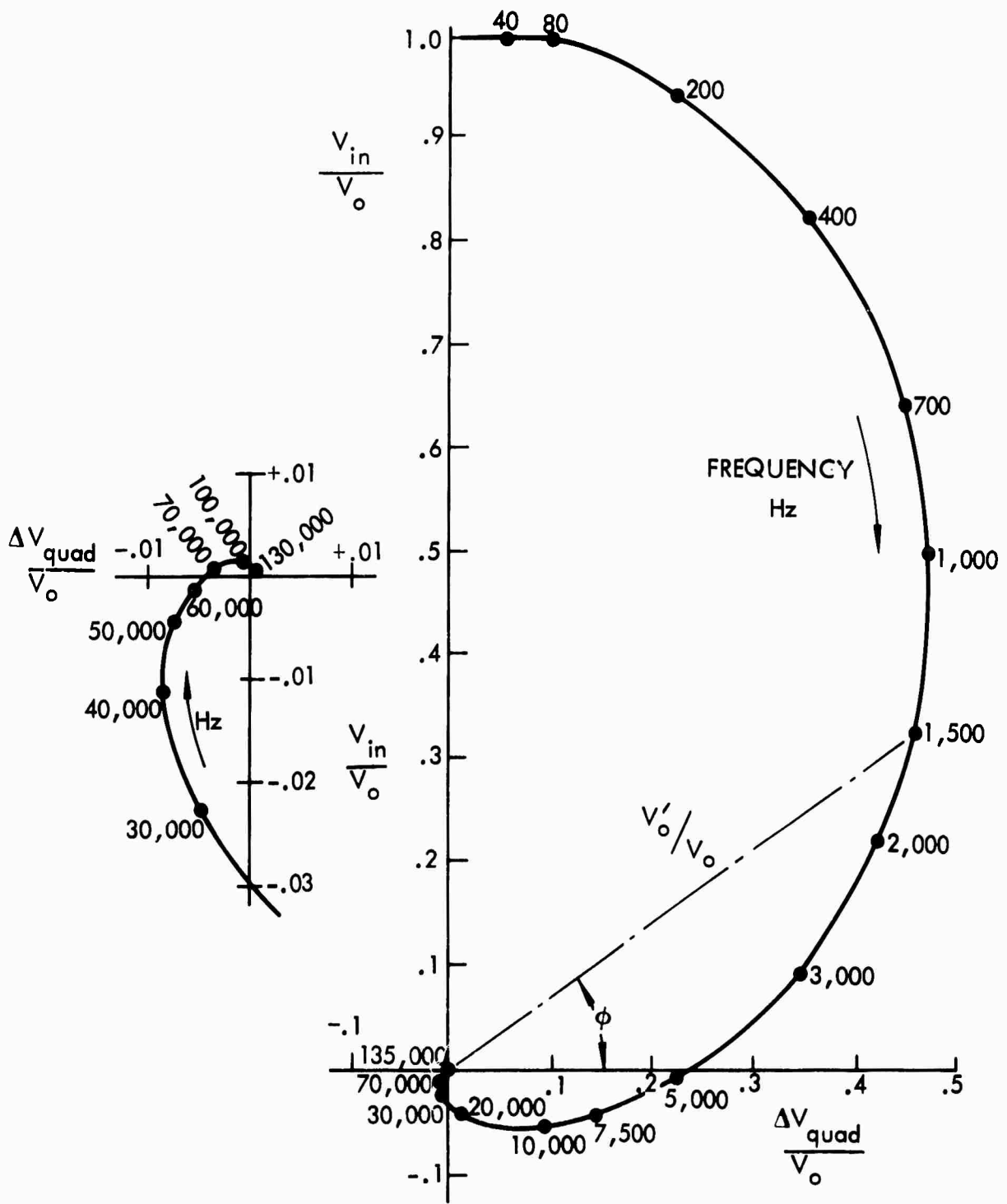


FIGURE 22 THROUGH TRANSMISSION EDDY CURRENT DATA

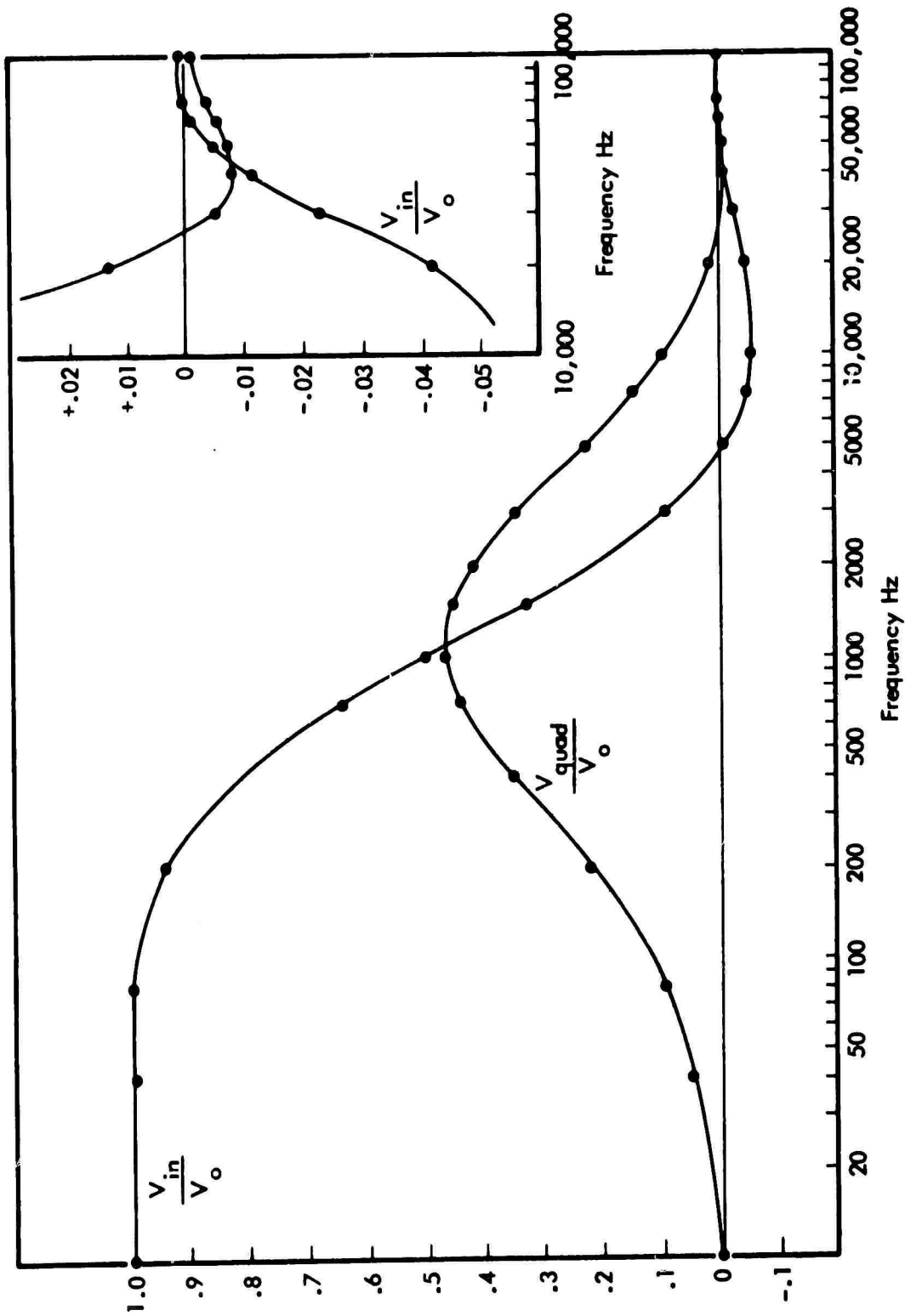


FIGURE 23 PARAMETRIC PLOT OF THROUGH TRANSMISSION EDDY CURRENT DATA

with the lock-in amplifier, the experimental points were determined with care. Amplitude ratios are accurate to within a percent and phase angles are accurate to within one degree. Figures 24 and 25 are plots of V_{in}/V_o and V_{quad}/V_o vs. the frequency thickness product. Note that below a value of about 70 Hz-inch the frequency and thickness may be varied at will without affecting the received eddy current signal, as long as the product of the two is maintained constant. Above this value, the separation of the curves shows that this is not true. This upper bound is worth noting because some of the older theories⁽³⁾ indicate that the "frequency thickness product rule" holds throughout the frequency range in which eddy current tests might be performed.

In order to be sensitive, the electronics in almost any eddy current system must be able to detect small changes in a large sinusoidal signal. This can be accomplished by performing an electrical cancellation of the majority of the signal and passing the remainder into an amplifier at high gain. To see a one per cent change in a signal, one could cancel out approximately 99 per cent of the signal and increase the amplifier gain to just below saturation. High gain operation cannot be used without electrical cancellation because the amplifiers would be strongly over-driven.

The cancellation is usually accomplished with an AC bridge. Through transmission systems use a mutual inductance bridge or comparison coils (which amount to the same thing). Use of the lock-in amplifier makes it possible to accomplish signal cancellation by phase sensitive detection. Rather than balancing a bridge, one adjusts the lock-in amplifier so that it senses voltages at right angles to the large signal which must be cancelled. Since the component of a voltage at right angles to itself is zero, the output of the system approaches zero, and the output may be observed at high gain. This means of obtaining sensitivity is used in the thickness measurement applications described in a later section. This procedure is quick and convenient when using the lock-in amplifier for through transmission testing because one need not construct and balance an AC bridge.

Because the lock-in amplifier is continuously adjustable from 1.5 Hz to 150 KHz it is possible to select optimum operating frequencies for a given application. Most eddy current systems are not strongly frequency sensitive but it is beneficial to be able to select ranges of operating frequency. Using the lock-in amplifier for through transmission eddy current testing of a variety of materials, we have been able to determine frequencies at which there exists a linear relationship between the thickness and the eddy current signal. Examples appear in the next section.

The frequency dependence of the phase shift experienced by an electromagnetic wave in a conducting medium can be readily calculated. If the field at the front face of a metal sheet of thickness d is $B_o \cos(kx - \omega t)$, then the field at the far side of the sheet is $B_o \cos(k(x + d) - \omega t)$, from which it can be seen that the phase shift is $\phi = kd$.

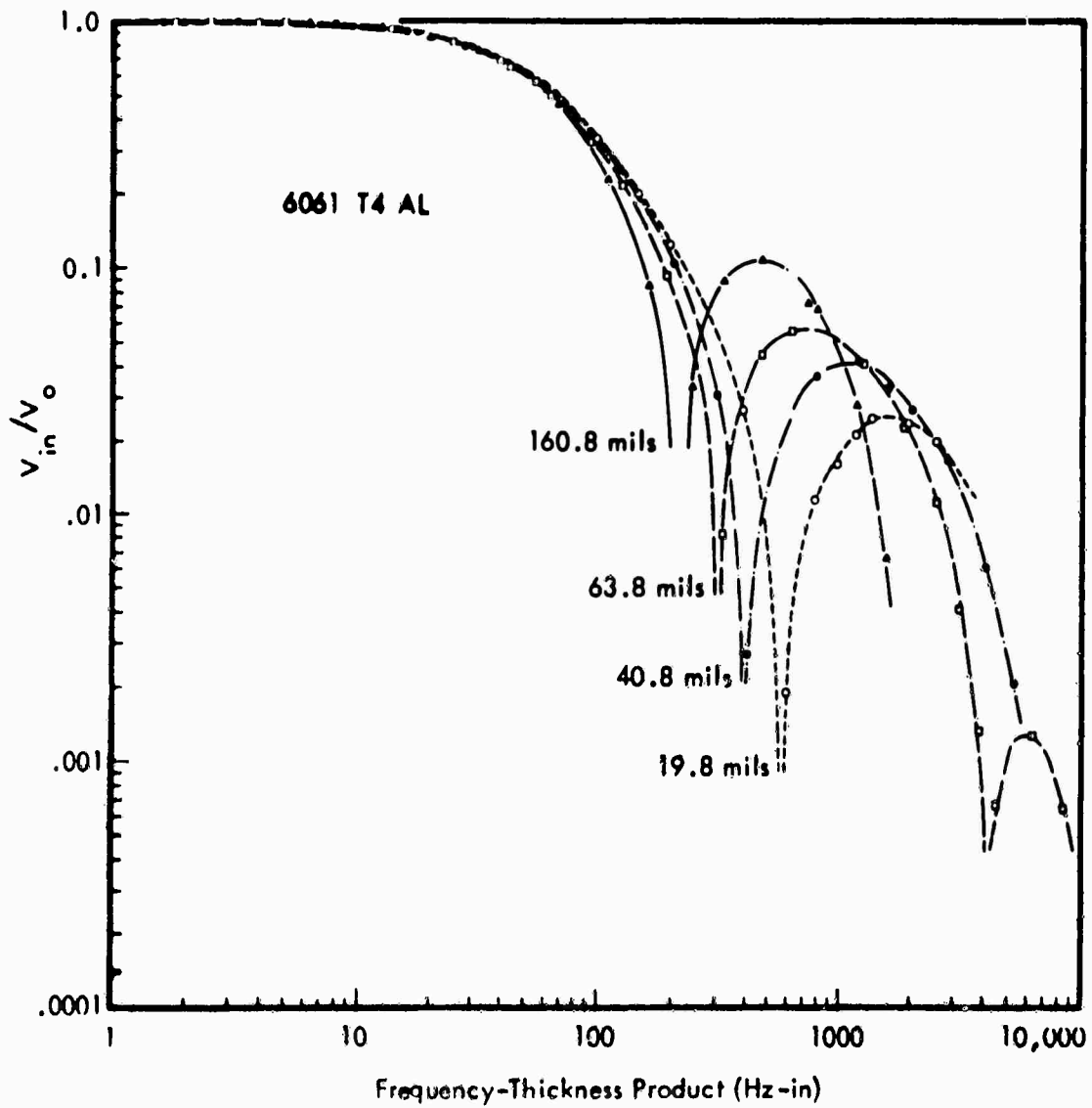


FIGURE 24 THROUGH TRANSMISSION EDDY CURRENT DATA IN TERMS OF FREQUENCY THICKNESS PRODUCT — V_{in} vs. ($f t$)

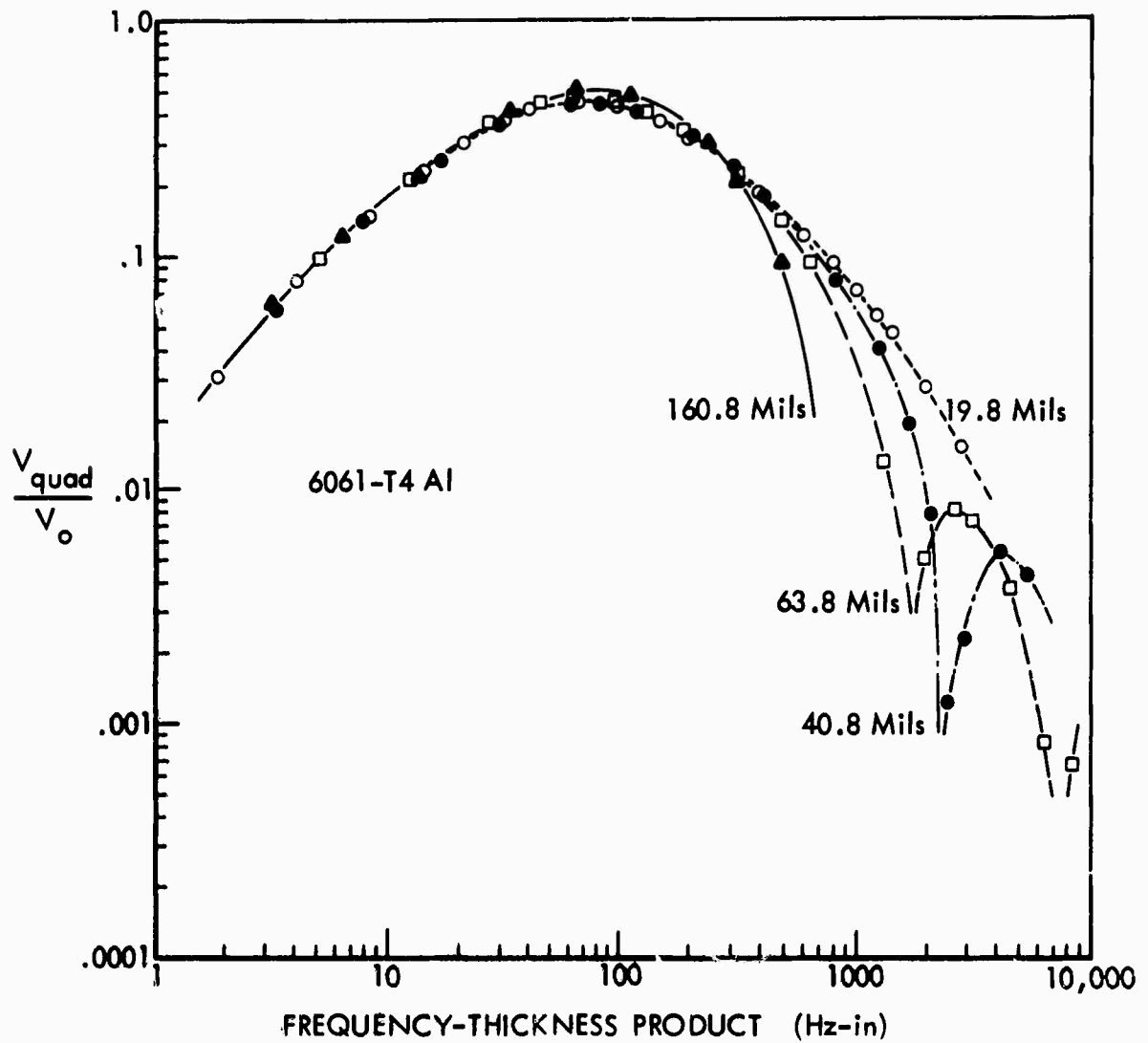


FIGURE 25 THROUGH TRANSMISSION EDDY CURRENT DATA IN TERMS OF FREQUENCY THICKNESS PRODUCT — V_{quad} vs. (ft)

Using a standard result for the wave number⁽⁴⁾,

$$k = \frac{\omega}{c} \left[1 + \left(\frac{4\pi\sigma}{\omega} \right)^2 \right]^{1/4}$$

one obtains, to good approximation, $\phi = \frac{2\pi}{c} \sqrt{2\sigma} d \sqrt{f}$. The con-

ductivity of the medium is σ , the eddy current frequency is f , and c is the velocity of light. This expression provides a theoretical curve which can be compared to the through transmission eddy current data. The results of that comparison for a piece of 63 mil 6061-T4 aluminum appear in Figure 26. Quantitative data of the type discussed here provides a medium for communication between eddy current investigators and improves ones understanding of the operation of through transmission eddy current systems. Greater understanding can shorten the time for system design, and create greater confidence in final test procedures.

THROUGH TRANSMISSION THICKNESS MEASUREMENT APPLICATIONS

Chemical Milling Thickness Monitor

Theory

A through transmission eddy current system has been used to monitor a titanium chemical milling operation⁽⁵⁾. Through transmission eddy current was selected for this purpose because no contact with the test part is necessary and measurements can be made down to the tenth mil range. Use of a lock-in amplifier in the system allowed easy determination of the required operation frequency for linearity, and allowed a quick evaluation of the system without building bridge circuitry.

Apparatus

Figure 21 is a block diagram of the electronics and Figure 27 is a photograph of the equipment. The electronics for this experiment is identical to that used in the last section. The test coils were contained in glass test tubes to protect them from the etchant solution and were mounted in the usual through transmission configuration. Figure 28 is a closeup of the test coils. The etchant was a weak solution of hydrofluoric and nitric acids in water. It is essential that there be no contact between the acid bath and the eddy current coils. Although glass tubes were used for insulation in the present experiment, light weight plastic tubes would be more durable in practice.

The system described here could act as the final shop configuration or could serve as the basis for design of an inexpensive special purpose system. The final inspection system should have a variable frequency capability because different operating frequencies will be necessary to obtain a linear dependence of eddy current signal on part thickness for different materials and thickness ranges.

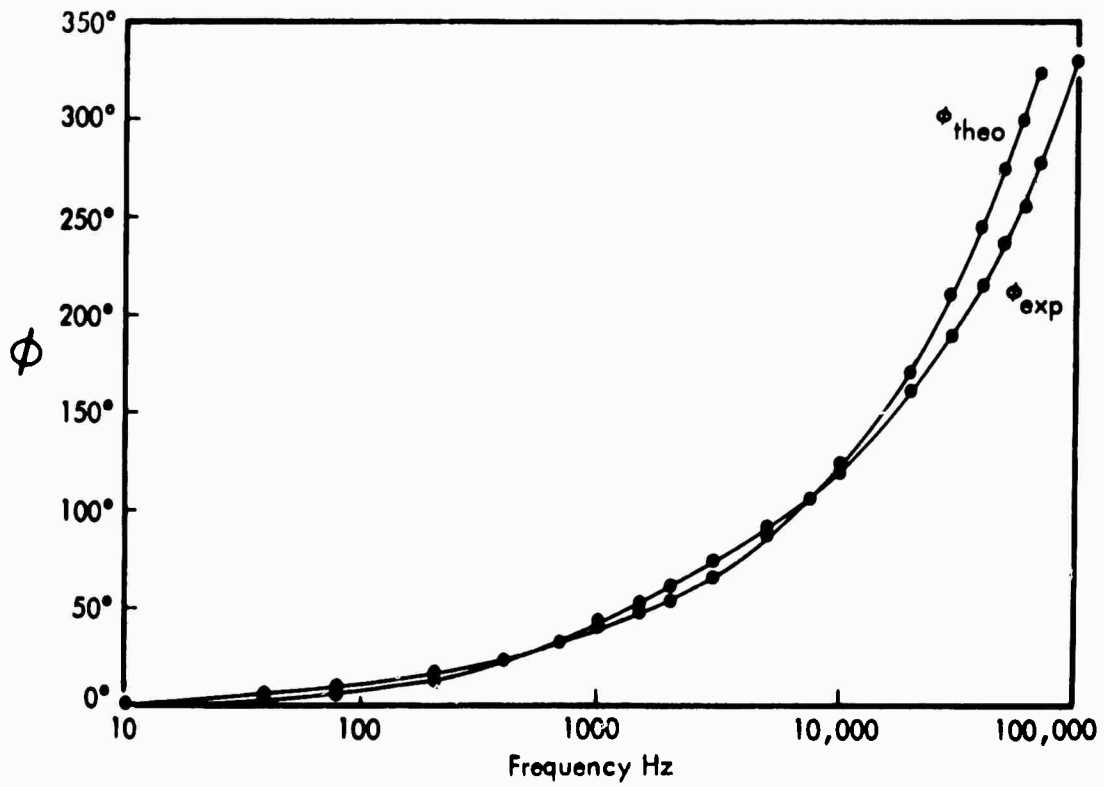


FIGURE 26 THROUGH TRANSMISSION DATA COMPARED WITH THEORY

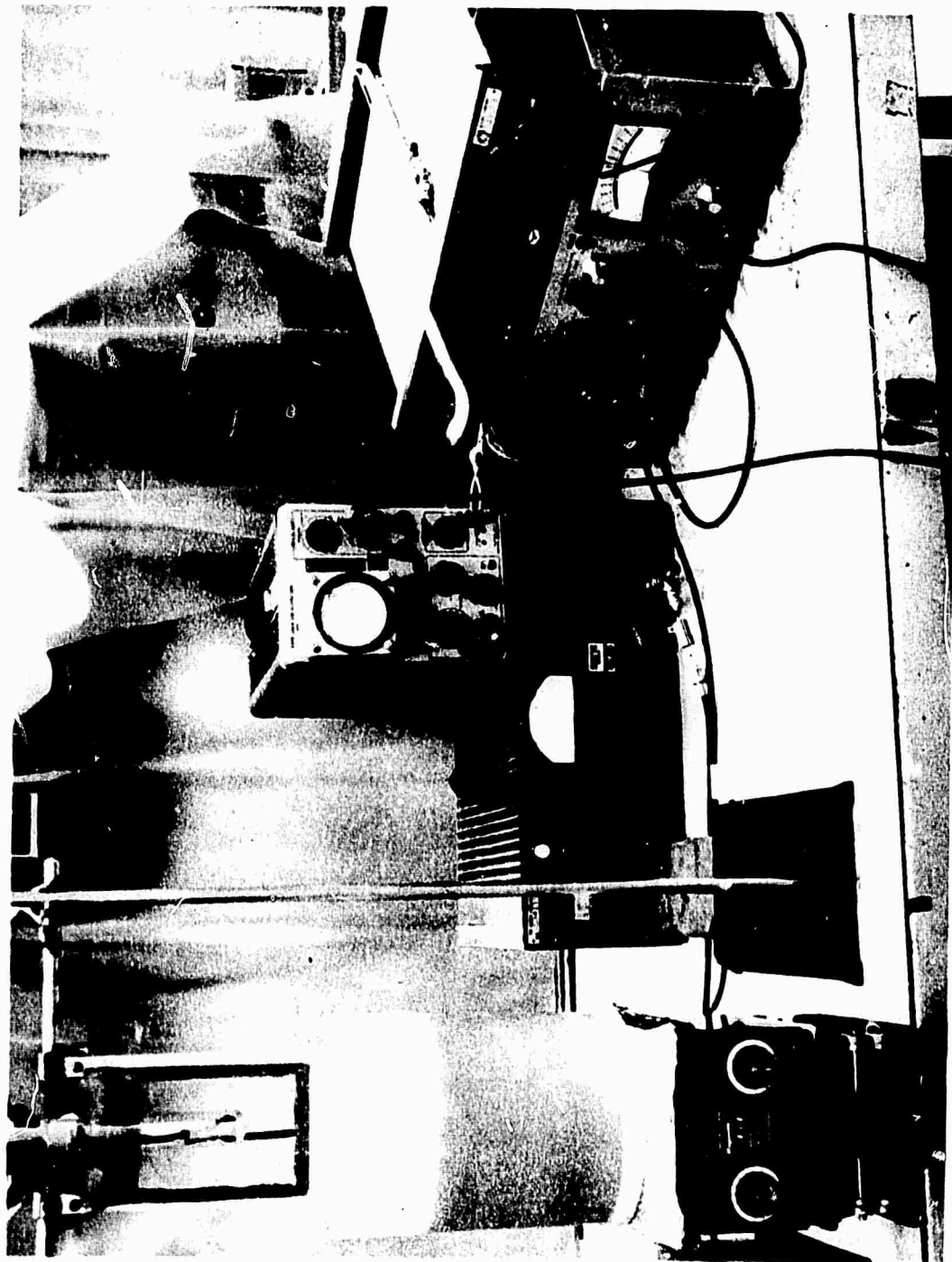


FIGURE 27 APPARATUS FOR CHEMICAL MILLING THICKNESS MONITOR



FIGURE 28 TEST COIL ARRANGEMENT FOR CHEMICAL MILLING THICKNESS MONITOR

Data and Conclusions

For the present milling experiment it was desired to obtain a linear relationship between eddy current signal and thickness for titanium panels between zero and forty mils thickness. The lock-in amplifier was adjusted to read V_{quad} , i.e., voltage at right angles to the pickup signal V_o with test part absent. A frequency of 4000 Hz produced the desired linearity and an eighty point calibration curve was prepared which appears in Figure 29. Proper frequency selection is important because at a frequency of 20,000 Hz, for example, the linearity exists between zero and fifteen mils only.

A test part was placed into position and the milling process initiated. Use of the calibration curve allowed an X-Y recorder to be adjusted so that a curve of thickness vs. time was automatically recorded. The result appears in Figure 30. Although the test part was entirely etched away the thickness curve stops at 0.2 mil. This is because the outer periphery of the test part was not allowed to etch at all, so that a square "window", which affected the eddy current signal, remained after etching. This served as a reminder that, although the coils were one-half inch in diameter and one inch apart, the area sensed was about four inches square. Actually, for work of this kind, an average thickness obtained over several square inches is more desirable than a point measurement which may not be truly representative of the general area. Notice from Figure 30 that titanium thickness changes of one tenth mil are readily detectable.

A notable aspect of the system is the insensitivity of the eddy current thickness reading to part position. Figure 31 shows that the part can be placed anywhere between the test tubes protecting the coils with minimal error. This is significant because convection currents in the acid bath can cause the test part to drift back and forth between the coils. The system is insensitive to the presence of the conducting acid bath, and to turbulence and temperature fluctuations within the bath. Finely divided metal particles which can fill a small volume acid bath do not affect the eddy current results. Since no contact with the part is necessary, materials can be etched from both sides simultaneously.

There is some interest in monitoring the thickness uniformity of sheet materials before etching. The non-contact aspect of the through transmission system makes it particularly appropriate for scanning large sheets. An in motion thickness measurement is described in the next section.

Ribbon Thickness Monitor

Theory

A system was constructed to monitor the thickness of titanium ribbon that was to be exposed to chemical milling⁽⁶⁾. A through transmission system was considered because the non-contact characteristic allowed measurements to be made while

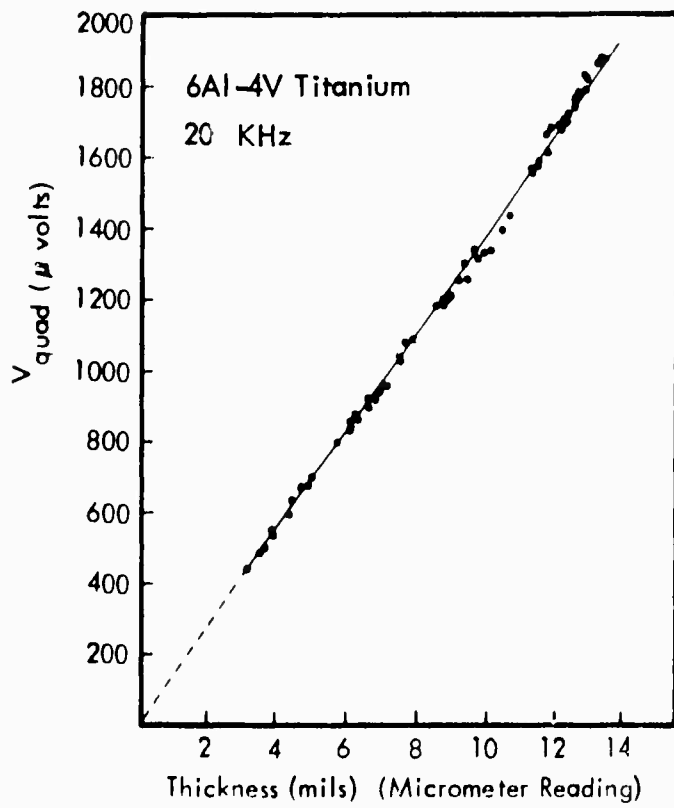


FIGURE 29 CALIBRATION CURVE FOR CHEMICAL MILLING PROCESS MONITOR

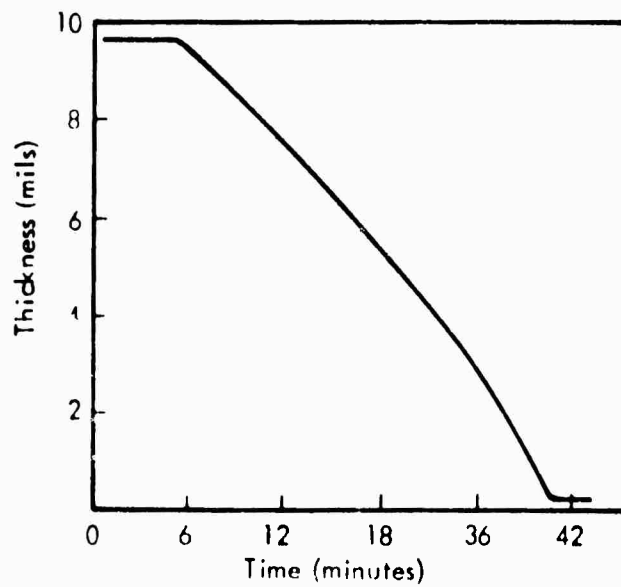


FIGURE 30 TITANIUM CHEMICAL MILLING THICKNESS DATA

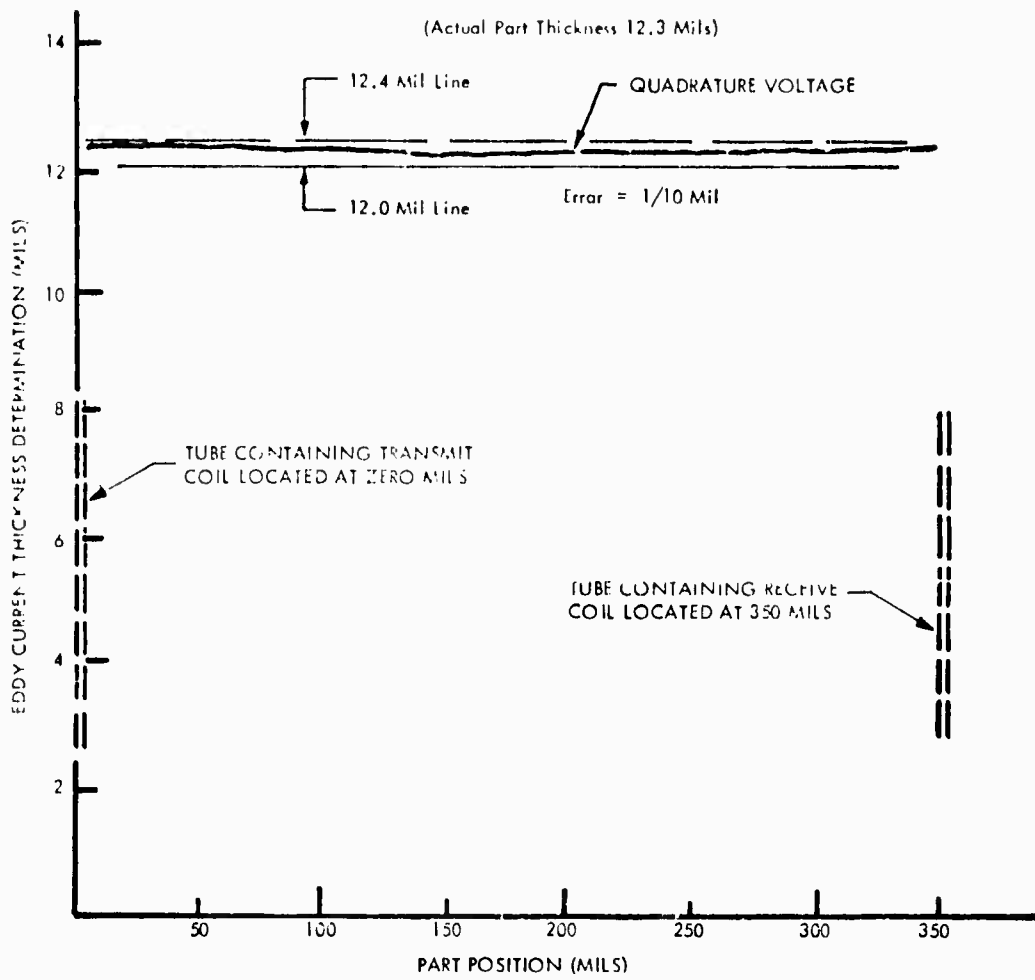


FIGURE 31 PART POSITION SENSITIVITY

the ribbon was in motion, and the part position insensitivity minimized error due to flutter. In addition, through transmission eddy current allowed the detection of small thickness changes about an average thickness.

Apparatus

The electronics is shown in Figure 32. Notice that no power amplifier is used; the entire system consists of the lock-in amplifier and two eddy current coils (although the pickup coil was matched through a 3K resistor to the input impedance of the HR-8 preamplifier). The lock-in amplifier will supply only 5 milliamps but both coils contain a large number of turns and adequate pickup signals were obtained. A photograph of the equipment appears in Figure 33. The nylon guide pictured there was employed so that the ribbon would pass properly between the coils. Because the coils sense an area larger than that presented by the ribbon it was necessary to constrain the ribbon so that it would not drift sideways.

Data and Conclusions

A section of ribbon 4.1 mils thick was passed between the coils and the lock-in amplifier was adjusted to sense the voltage, V_{quad} , at right angles to the signal received. This thickness of ribbon represented a maximum value and all subsequent measurements were made between 3.4 mils and 4.0 mils. A frequency of 150 KHz was selected. The calibration curve, showing a linear relationship between thickness and eddy current signal appears in Figure 34. This curve was used to calibrate a strip chart recorder and fifty feet of ribbon were monitored. The results appear in Figure 35. Thickness changes on the order of .02 mil were readily detected and recorded.

PHASE SENSITIVE EDDY CURRENT TESTING APPLIED TO BOLT HOLE CRACK DETECTION

Theory

Although ultrasonic methods are being developed for bolt hole crack detection there continues to be some interest in the application of eddy current to the inspection of bolt holes with the fastener removed. A representative sensitivity, at present, is the reliable detection of a 30 mil by 30 mil EDM slot in a 3/8 inch bolt hole in aluminum, and the occasional detection of a 15 mil by 15 mil EDM slot. Present systems are limited by noise due to probe fit up or "liftoff" and signals from non-crack conditions such as gouges and scratches. Since none of the systems being employed make use of all of the eddy current information available, experiments were carried out to determine whether or not amplitude and phase detection with the lock-in amplifier would increase sensitivity. While phase sensitive methods did improve sensitivity, it was found that displaying the time derivative of the amplitude signal produced equal improvements. If an inspection probe can be constructed which maintains contact between the coil and inner bolt hole surface by spring loading, a significant improvement could be obtained in the detection reliability of the 15 mil by 15 mil EDM slot by combining the two

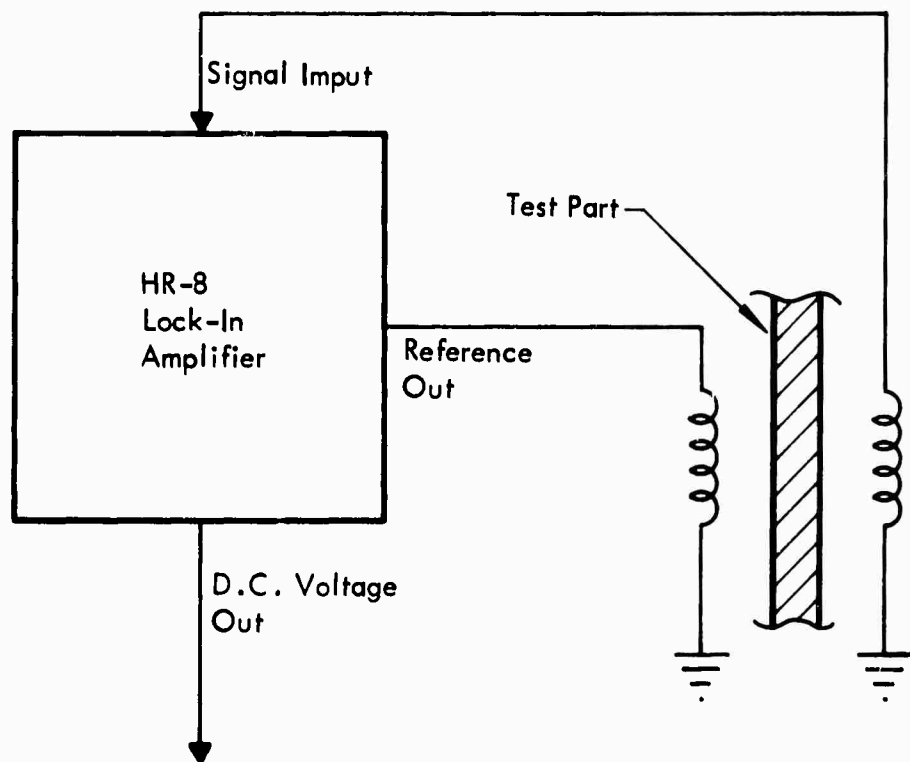


FIGURE 32 EQUIPMENT FOR RIBBON THICKNESS MONITOR

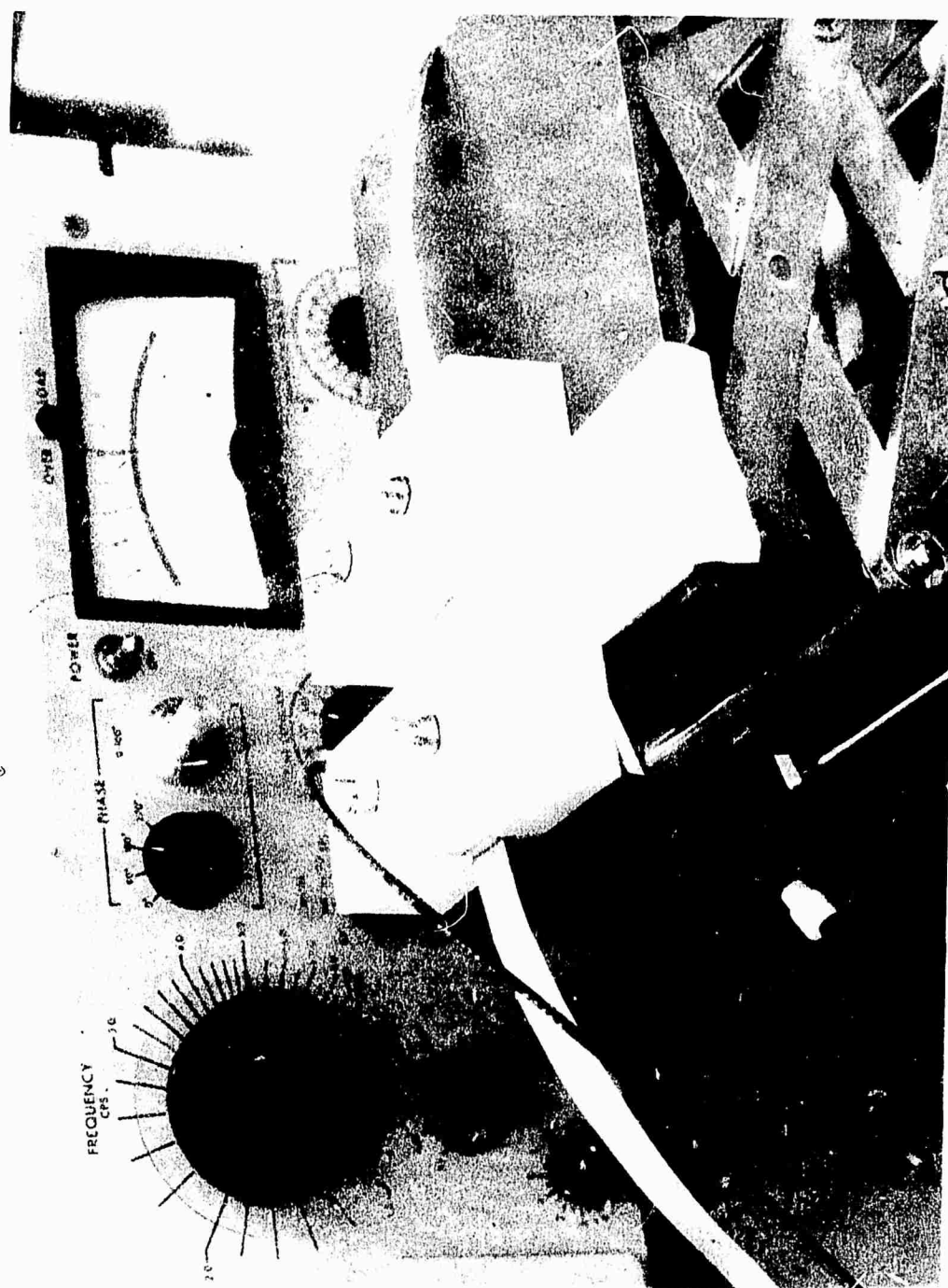


FIGURE 33 APPARATUS FOR RIBBON THICKNESS MONITOR

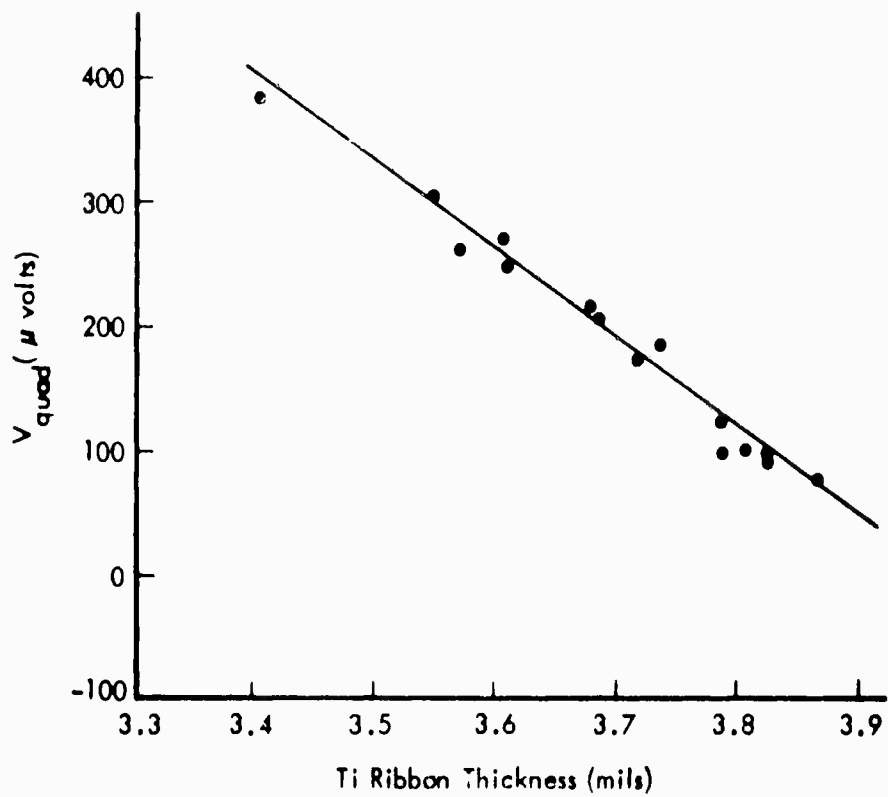


FIGURE 34 CALIBRATION CURVE FOR RIBBON THICKNESS MEASUREMENT

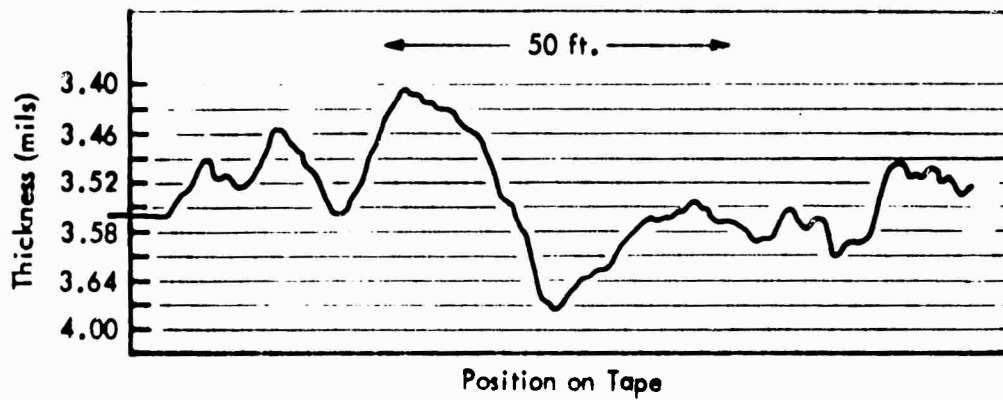


FIGURE 35 TITANIUM RIBBON THICKNESS DATA

methods and displaying the results on a CRT screen. There are several other processing and display procedures applicable to this problem and they will be discussed in detail below.

The inspector is making use of all the eddy current information available if his equipment senses both amplitude A , and phase ϕ changes. In the present experiment this information is obtained by the simultaneous measurement of V_{in} and V_{quad} using two lock-in amplifiers. Eddy current sensitivity is obtained by the bridge balance method. Data similar to that presented here was taken with the Nortec NDT-6 instrument⁽⁷⁾. The two sets of data appeared to be essentially equivalent. The Nortec instrument is portable and suitable for actual inspection use. The lock-in amplifier system is for laboratory use only, but is more flexible in the selection of operating frequency and coils. Some of the benefits of this flexibility are exhibited in the section entitled "Quantitative Eddy Current Testing".

Apparatus

Figure 36 is a circuit diagram of the equipment used and Figure 37 is a photograph of the apparatus. Although more refined bridges are used in most commercial instruments a conventional inductance bridge was adequate here. Two HR-8 lock-in amplifiers were used. One served as oscillator, fed the power amplifier, and triggered the other lock-in amplifier. The bridge output was fed to both amplifiers, one being adjusted to sense V_1 and the other being adjusted to sense V_2 , (which was 90 degrees out of phase with V_1). The outputs of the two instruments were fed to a CRT or X-Y recorder as required. The operation frequency was arbitrarily selected to be 100 KHz.

Figure 38 is a photograph of the test probe in position for inspection of a bolt hole. The coil itself has a diameter of 72 mils, is circular in shape, and contacts the inner surface of the bolt hole in the same manner in which a conventional pancake coil contacts a flat surface. One hundred percent inspection of a bolt hole interior is not practical with a coil this small. One normally settles for inspection of the edges where a crack is most likely to occur. The inspector could employ a larger coil, accepting the decrease in sensitivity in order to obtain total surface inspection, and still employ the signal processing techniques described below.

Data and Conclusions

Figure 39 shows the time derivative of the amplitude for various bolt hole conditions. The ten mil indication is easily lost in other kinds of noise. The 15 mil indication is fairly reliable although not really discernable from the gouge indication. This type of processing is the best way to obtain a needle deflection indication of the EDM slot.

Figures 40 and 41 contain both amplitude and phase information. The EDM slot indication is the curved spike which moves down and to the right. Again the 10 mil slot is easily lost in background noise, while the 15 mil slot is more reliably

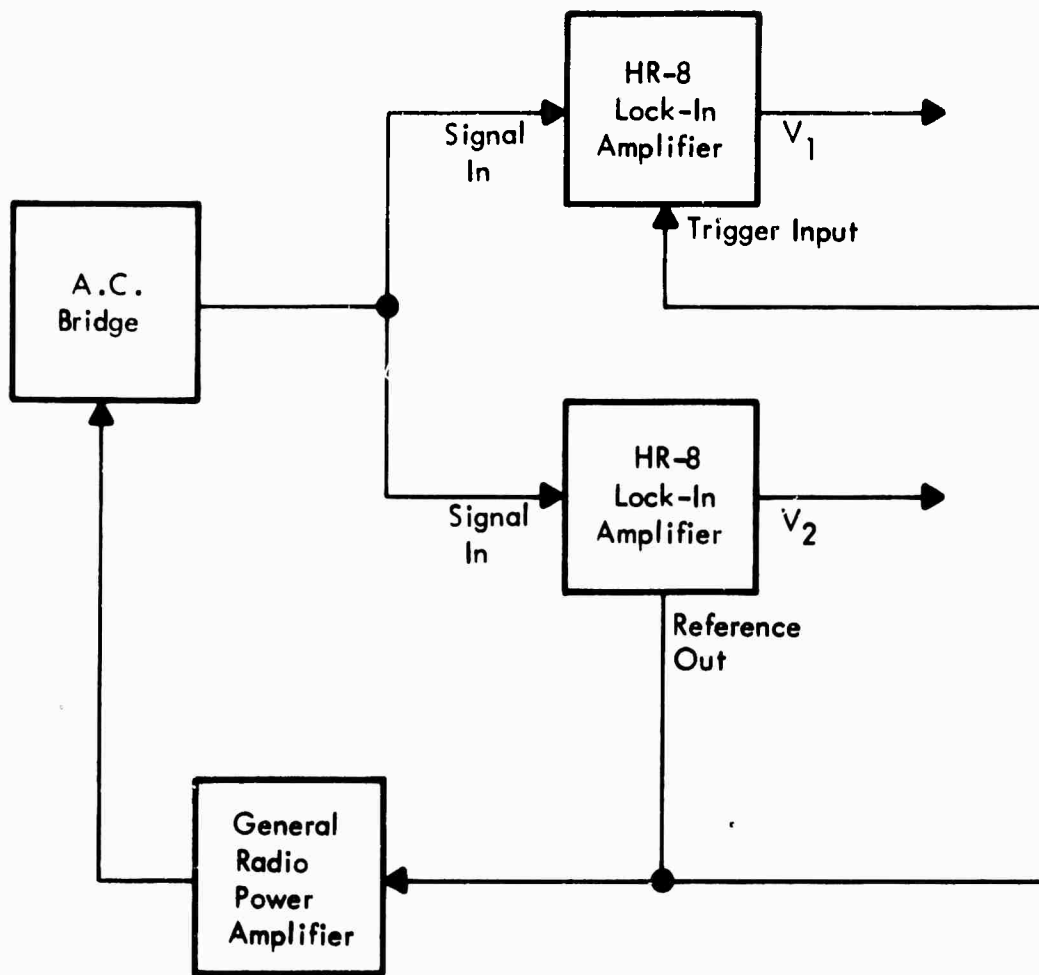


FIGURE 36 BLOCK DIAGRAM OF BOLT HOLE CRACK DETECTION EQUIPMENT

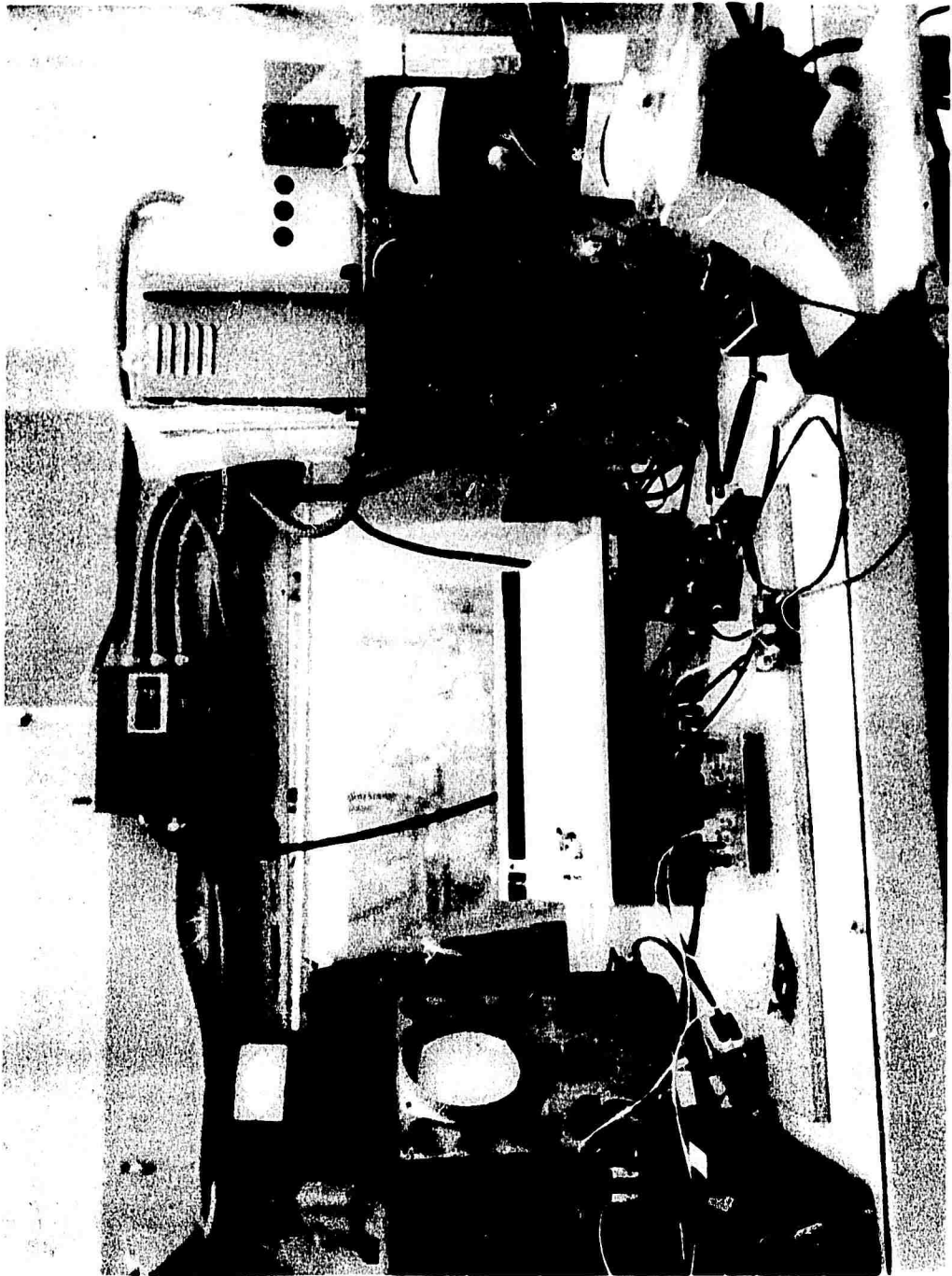
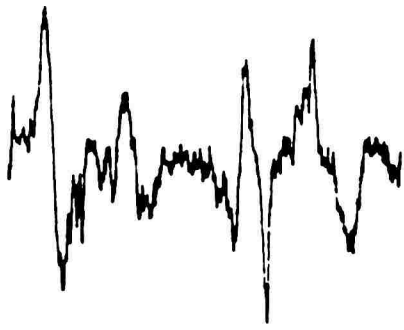


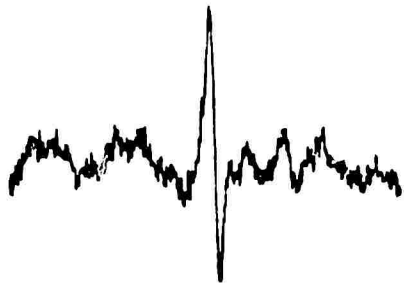
FIGURE 37 APPARATUS FOR BOLT HOLE CRACK DETECTION



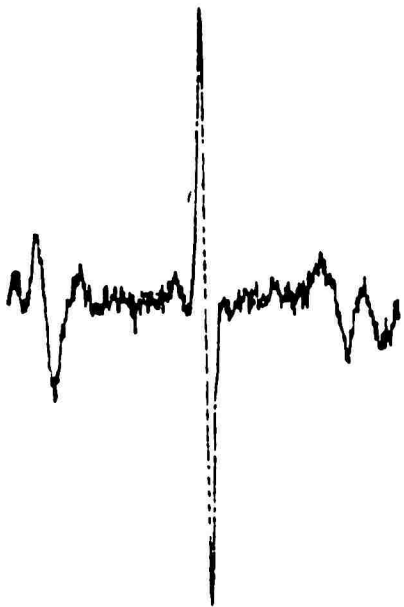
FIGURE 38 PROBE AND TEST PART FOR BOLT HOLE CRACK DETECTION



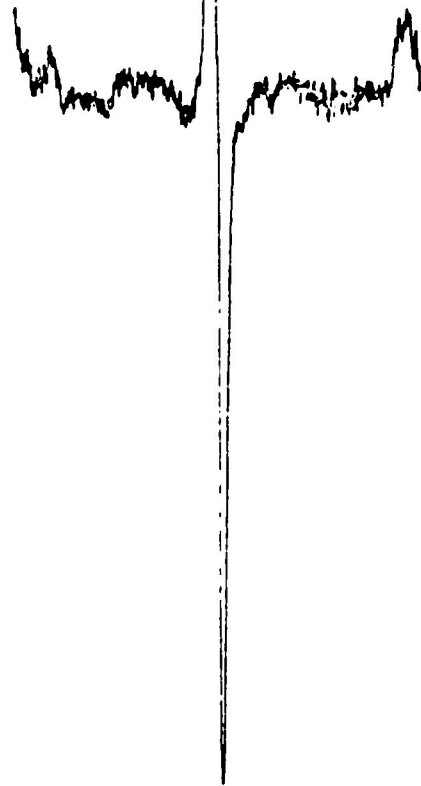
Gouge



10 mil



15 mil



30 mil

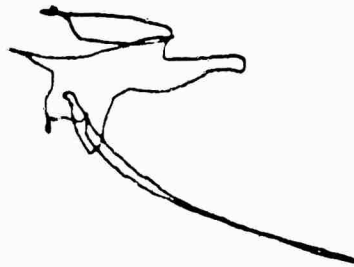


No Flaw

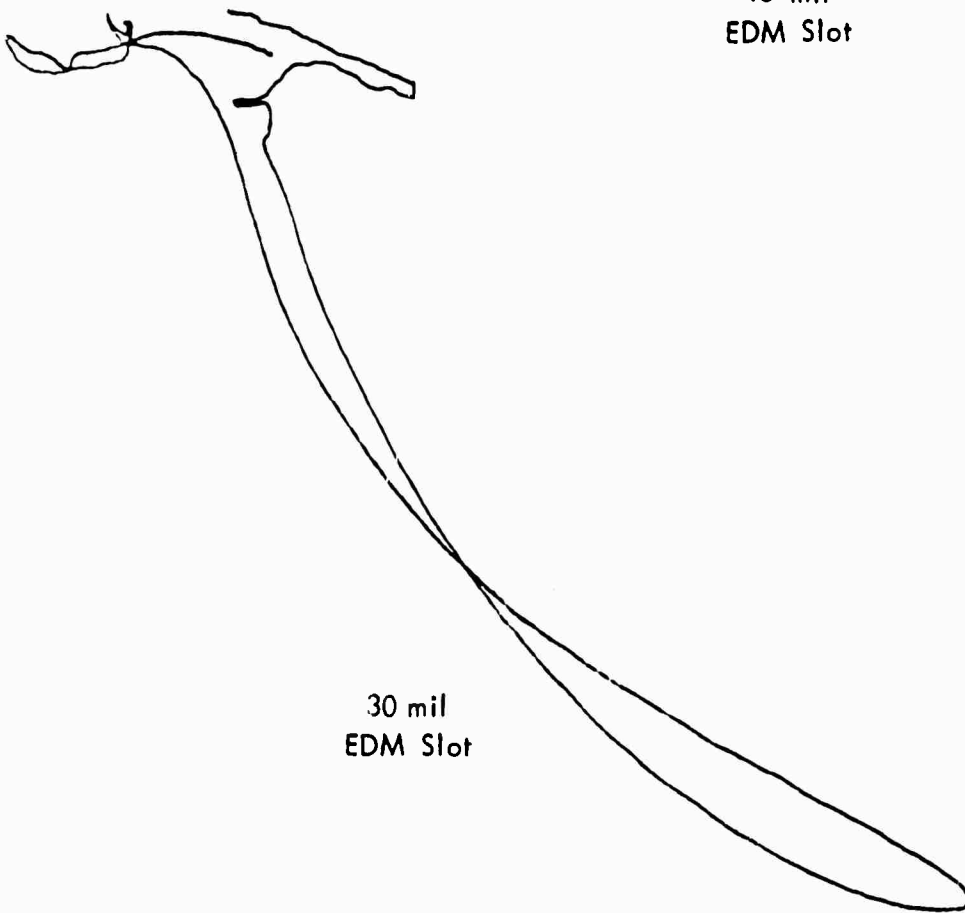
FIGURE 39 EDDY CURRENT BOLT HOLE INSPECTION
 dV/dt vs. t



10 mil
EDM Slot

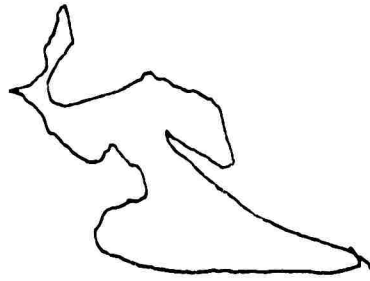


15 mil
EDM Slot

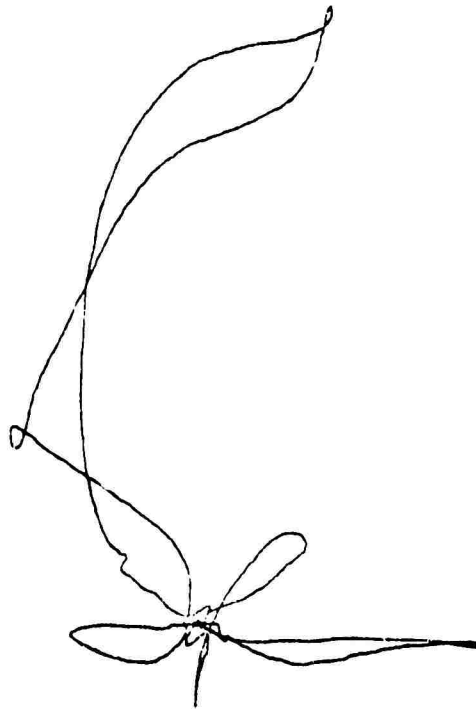


30 mil
EDM Slot

FIGURE 40 EDDY CURRENT BOLT HOLE INSPECTION V_1 vs. V_2



FLAW FREE



GOUGE

FIGURE 41 EDDY CURRENT BOLT HOLE INSPECTION V_1 vs V_2

detectable. Notice that the gouge is definitely discernable from the 15 mil slot because each has a characteristic shape. One can conclude that amplitude and phase analysis does increase the amount of information obtainable from the system, but large increases in sensitivity are not to be expected. Although the system can be adjusted to sense changes in any desired direction of the voltage plane it is impossible to "tune out" the noise because it clearly appears in all directions of the plane. The best procedure is to select a direction of the plane which gives the maximum flaw indication. It should be recognized that even the EDM slot indication has no single definite direction in the plane, and the reaction from a real crack will probably look different still. Thus it appears that the best way to assimilate data of this kind is to present the entire pattern, as we have here, on a CRT or X-Y recorder, and leave the pattern recognition to the inspector.

Figure 42 includes both differentiation and amplitude and phase analysis. The data is appropriate for CRT presentation. Flaws take on the characteristic "bow tie" shape seen in the diagram. If techniques such as these fail to significantly increase sensitivity they may still improve detection reliability.

QUANTITATIVE EDDY CURRENT TESTING

Single Coil Tests

Theory

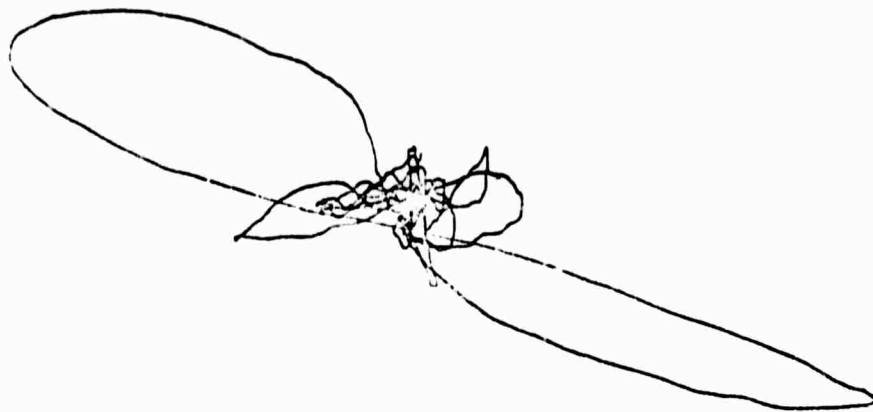
When an eddy current coil is placed on a test specimen it experiences a change in resistance and inductance. A complete description of all changes in the coil is contained in a plot of X/X_0 vs. $\Delta R/X_0$. X_0 is the inductance of the coil in air, X is the inductance of the coil on the test part and ΔR is the change in resistance experienced by the coil when it is placed upon the part. The use of ΔR rather than R , the resistance of the coil on the test part, has been common for some time in eddy current work. Data of this kind is normally collected by bridge balance techniques. In the present section a procedure is described for the collection of such data from bridge out-of-balance voltages. This procedure allows quantitative data to be automatically collected and recorded as the eddy current probe scans over the test part. A system of this kind significantly shortens the length of time required to collect quantitative data for a complex eddy current interaction.

Calibrated resistance and inductance data can be obtained from bridge out-of-balance voltages using equipment of the type appearing in Figure 43. It will now be shown how ΔX and ΔR information can be derived from the bridge output. Using complex notation, each lock-in amplifier sees a voltage $V = I_2 Z_2 - I_1 Z_1$. Using the complex ohms law to eliminate the current variables we obtain,

$$V = V \frac{Z_B}{2Z_R + Z_B} \left[\frac{Z_2}{Z_2 + Z_4} - \frac{Z_1}{Z_1 + Z_3} \right] \text{ where } Z_B = \frac{(Z_1 + Z_3)(Z_2 + Z_4)}{Z_1 + Z_2 + Z_3 + Z_4}$$



10 mil
EDM Slot



15 mil
EDM Slot

FIGURE 42 EDDY CURRENT BOLT HOLE INSPECTION

$$\frac{dV_1}{dt} \text{ vs. } 5 \frac{dV_2}{dt}$$

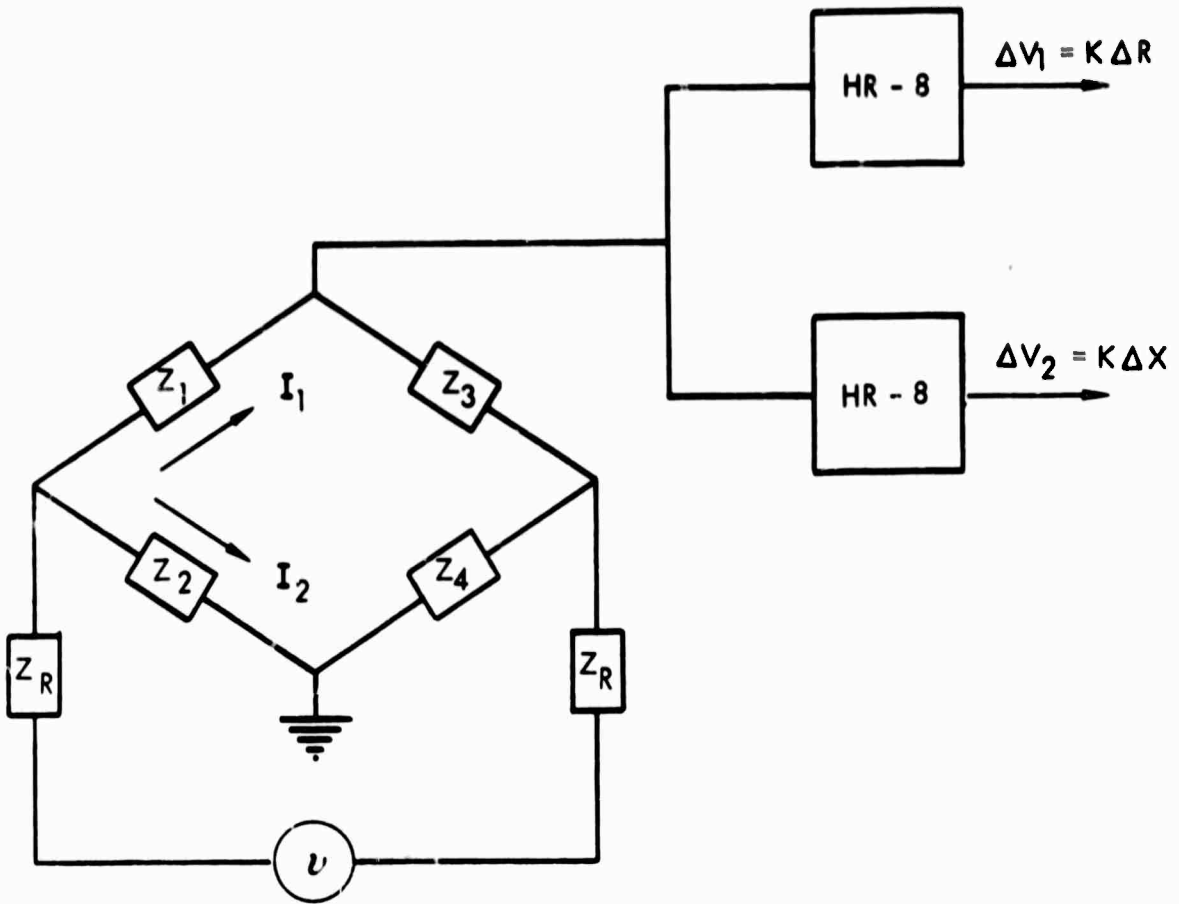


FIGURE 43 GENERALIZED EDDY CURRENT BRIDGE

Let the test coil be located in arm 2, and load arms 1 and 3 with extra resistance so that,

$$Z_1 \gg Z_2, Z_4$$

$$Z_3 \gg Z_2, Z_4$$

We then have,

$$V = \frac{V}{2Z_R} \left[Z_2 - Z_1 \frac{Z_2 + Z_4}{Z_1 + Z_3} \right]$$

Assuming the power amplifier to be a constant voltage source, the change in V due to the change in coil impedance Z_2 as the probe contacts the part is,

$$\Delta V = \frac{V}{2Z_R} \left[1 - \frac{Z_1}{Z_1 + Z_3} \right] \Delta Z_2$$

For a sinusoidal signal $V = A e^{j\omega t}$ and $Z_2 = R + jX$. Also denote,

$$\frac{1}{2Z_R} \left[1 - \frac{Z_1}{Z_1 + Z_3} \right] = k e^{j\alpha} \quad \text{which is constant.}$$

We then have,

$$\Delta V = A k e^{j(\omega t + \alpha)} [\Delta R + j \Delta X]$$

Taking the real part,

$$\Delta V = A k \Delta R \cos(\omega t + \alpha) + A k \Delta X \cos(\omega t + \alpha + \pi/2)$$

Adjusting the reference signal of one lock-in amplifier to be in phase with the first term and that of the second to be 90 degrees in advance we obtain,

$$V_1 = A k \Delta R = K \Delta R$$

$$V_2 = A k \Delta X = K \Delta X$$

Of course it is also necessary that the two amplifiers be operating at the same gain. Note that it has not been necessary to assume that the bridge is balanced before the coil impedance change occurred. It has been noticed experimentally that, if the calibration procedure is properly followed, the measured values of ΔR and ΔX are not affected by operating the bridge in an out of balance condition. It should also

be noted that if Z_R is too small the power amplifier will not act as a constant voltage source.

By noting the linearity between bridge out of balance amplitude A , and changes in impedance ΔZ_2 of bridge arm 2 one can experimentally verify that Z_1 and Z_3 are sufficiently large. Linearity is expected because,

$$\begin{aligned}\Delta A &= \sqrt{(\Delta V_1)^2 + (\Delta V_2)^2} \\ &= K\sqrt{(\Delta R)^2 + (\Delta X)^2} \\ &= K\Delta Z\end{aligned}$$

The check is accomplished experimentally, by inserting a General Radio decade resistor in arm 2, and plotting a graph of ΔA vs. ΔZ . Since the resistances are wire wound, known resistances and unknown inductances are being switched into the bridge. To establish linearity using the above formula however, it is only necessary that equal increments of impedance be switched in at each turn of the decade resistor knob, and it is necessary that the actual value of the impedance increment be known. For the values of Z_1 and Z_3 used in the present work this test has been performed and the linearity observed.

Apparatus

A block diagram of the equipment used for the collection of quantitative eddy current data appears in Figure 44. One phase was measured with a lock-in amplifier and the other with a boxcar integrator. This was done to exhibit the fact that both devices are capable of performing phase sensitive detection of a continuous wave signal. The boxcar integrator is generally used for the gated detection of pulsed signals. Less complex equipment configurations should be possible. Some initial experiments have been performed using a single boxcar integrator to produce both ΔR and ΔX data.

The Precision E - 310 serves as signal source. Power is coupled into the bridge through a transformer so that a single ended bridge output can be provided for coupling to the lock-in amplifier. The bridge output signal experiences band pass amplification in the HR-8, and then passes to the boxcar integrator for phase sensitive detection. The other phase sensitive detection channel is within the HR-8 itself. The trigger signal passes through the boxcar integrator first and then to the HR-8. The oscilloscope was replaced by an X-Y recorder when permanent recordings were desired.

The bridge circuitry is shown in Figure 45. With the exception of the "plug in" unit the bridge is similar to that used in several commercial instruments. The bridge can

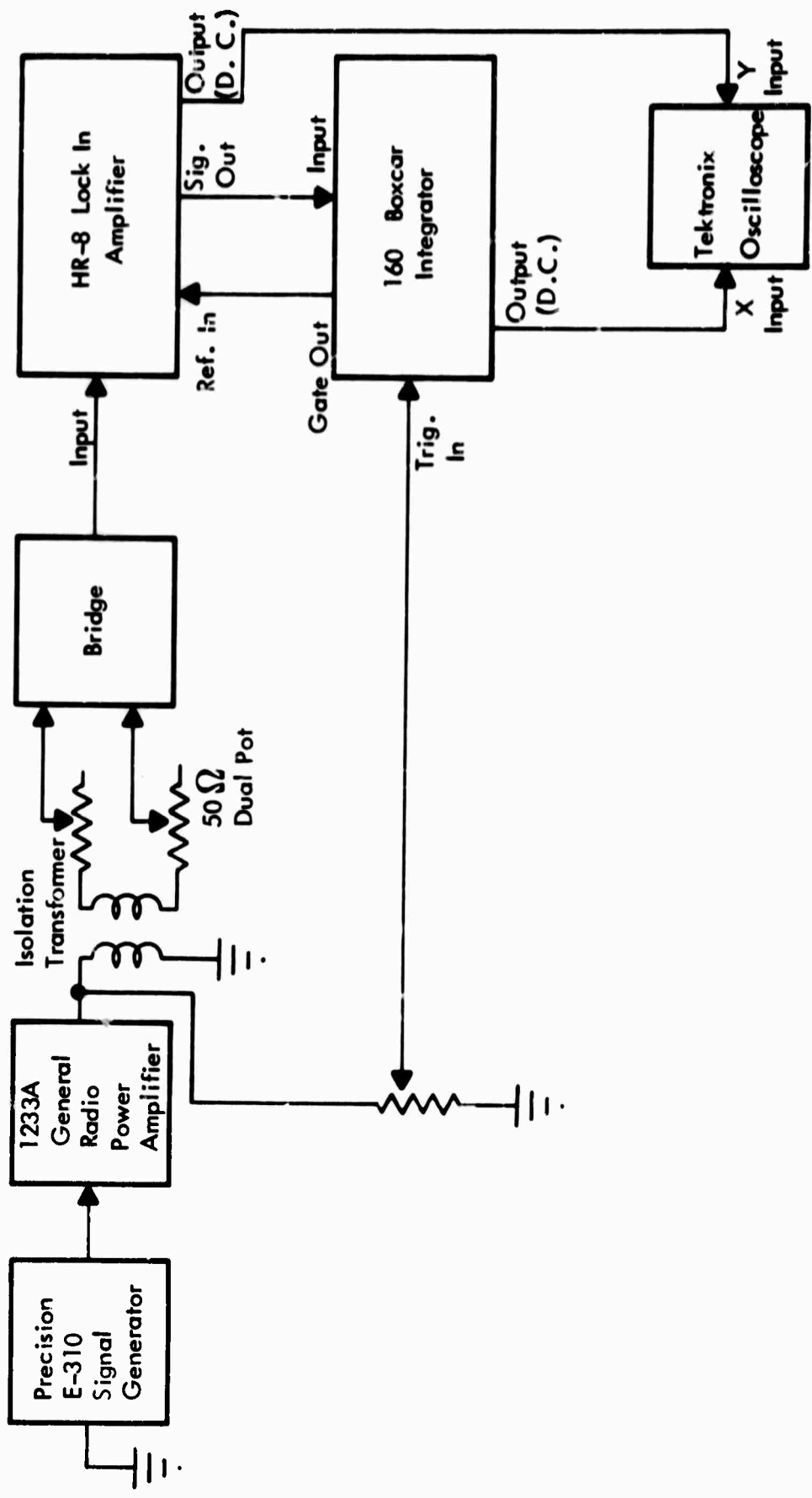


FIGURE 44 ELECTRONICS FOR COLLECTION OF QUANTITATIVE
EDDY CURRENT DATA

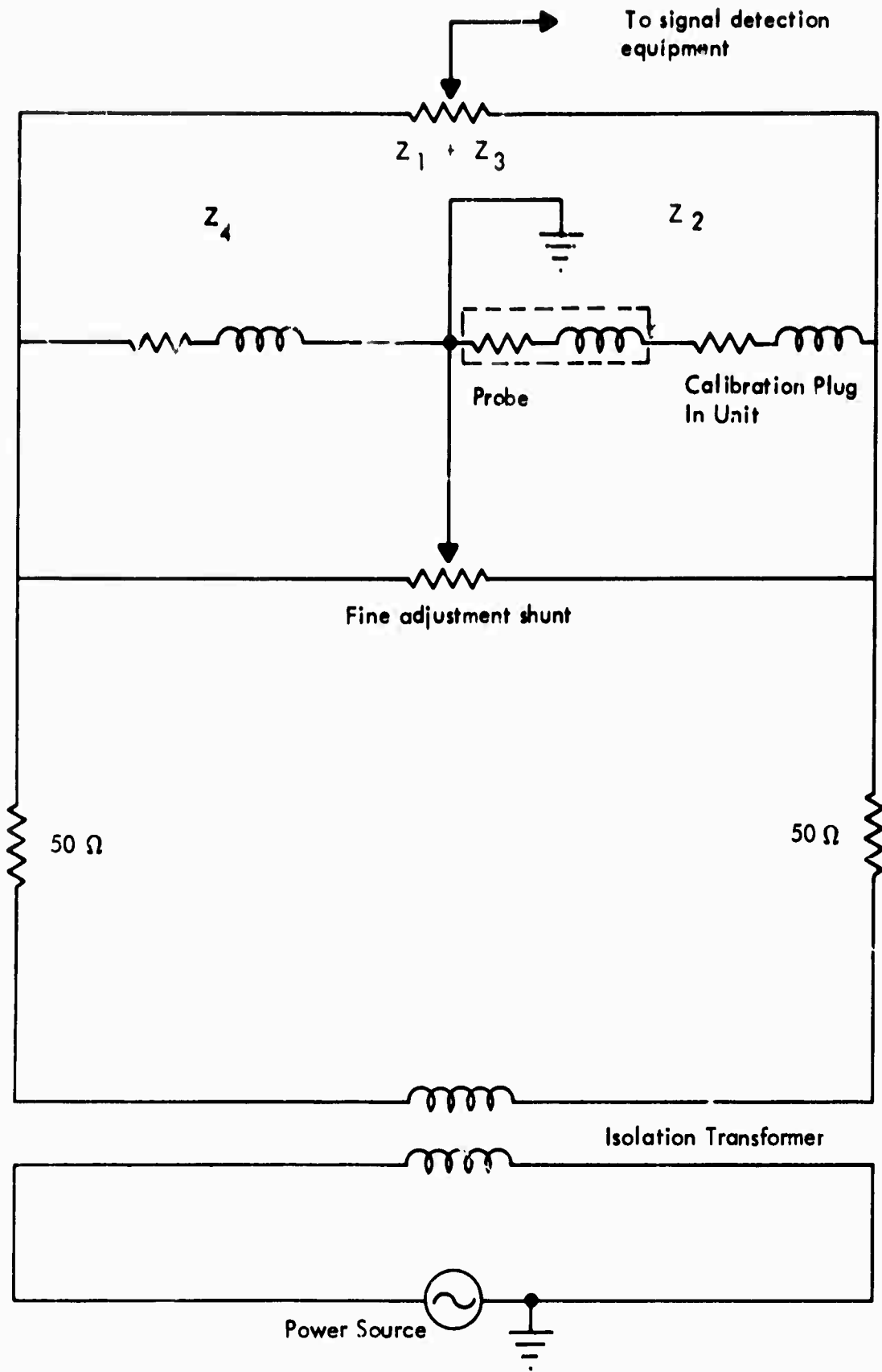


FIGURE 45 ERIDGE CIRCUIT FOR CALIBRATED IMPEDANCE PLANE DATA

be redrawn and put in the same form as that of Figure 43. Once in this form, it can be seen that the calculation of the previous section applies to the present bridge as long as the fine adjustment shunt is large compared to Z_2 and Z_4 . Typical values of Z_2 and Z_4 range from 1 to 3 ohms. Both the shunt resistance and $Z_1 + Z_3$ have been selected to be approximately 1000 ohms. The variable resistors are usually ten turn potentiometers.

The plug-in unit is used for the calibration of the equipment. Essentially, calibration is accomplished by adjusting the gain and phase of each phase sensitive channel so that a known impedance change ΔZ_2 , produces the proper deflection of an X-Y recorder pen. The impedance change is produced by inserting an impedance of known value into the plug-in unit. A piece of graph paper, marked off in calibrated axes and inserted into the X-Y recorder, determines whether or not the proper pen deflection has occurred. If, for instance, the known impedance change is 0.5 ohm, then adjustments are made so that the pen deflects along the $\Delta R/X$ axis a distance corresponding to 0.5 ohms. As long as the two channels are operating at the same gain and are 90 degrees out of phase, both the ΔR and ΔX axes are simultaneously calibrated using a pure resistance plug-in unit. The validity of this procedure depends upon the relations, $V_1 = K\Delta R$ and $V_2 = K\Delta X$, which have been shown to hold for the present bridge circuit.

The plug-in impedances vary from 0.01 ohm to several tenths of an ohm as measured by bridge balance techniques. The use of short lengths of resistance wire formed into the shape of a semicircle allowed nearly pure resistive impedance changes to be produced in the bridge. This was convenient because it allowed ready adjustment of the ΔR axis. The ΔX axis is then 90 degrees in advance of this axis. The plug-in resistances are durable and easily made. Banana plug connectors were found to be adequate for their construction. Variations in contact resistance at the connectors was less than ± 0.002 ohms.

Data and Conclusions

A Nortec NDT-3 is being used in this laboratory to detect the quantity of aluminum brazing material in titanium honeycomb parts⁽⁸⁾. The coil being used was balanced into the bridge described above and measurements were made of the impedance changes experienced as it scanned over the honeycomb face sheet. The results were automatically recorded on an X-Y plotter as the scanning operation took place. The data appeared as a plot of X/X_0 vs. $\Delta R/X_0$. All data was collected at 100 KHz. Figure 46 shows the location of the coil on the impedance plane as it scans over a single cell of the honeycomb panel. The points corresponding to lead, brass, aluminum, and copper are included in order to provide a reference background and to exhibit the fact that the present data is similar to conventional bridge balance data. Figure 47 is a more detailed look at the impedance changes induced in the test coil as it scans over the aluminum brazed titanium honeycomb panel. To produce this data the gain of the instrument was increased and a lower resistance plug-in impedance was used. When the coil center is located over a cell wall the coil

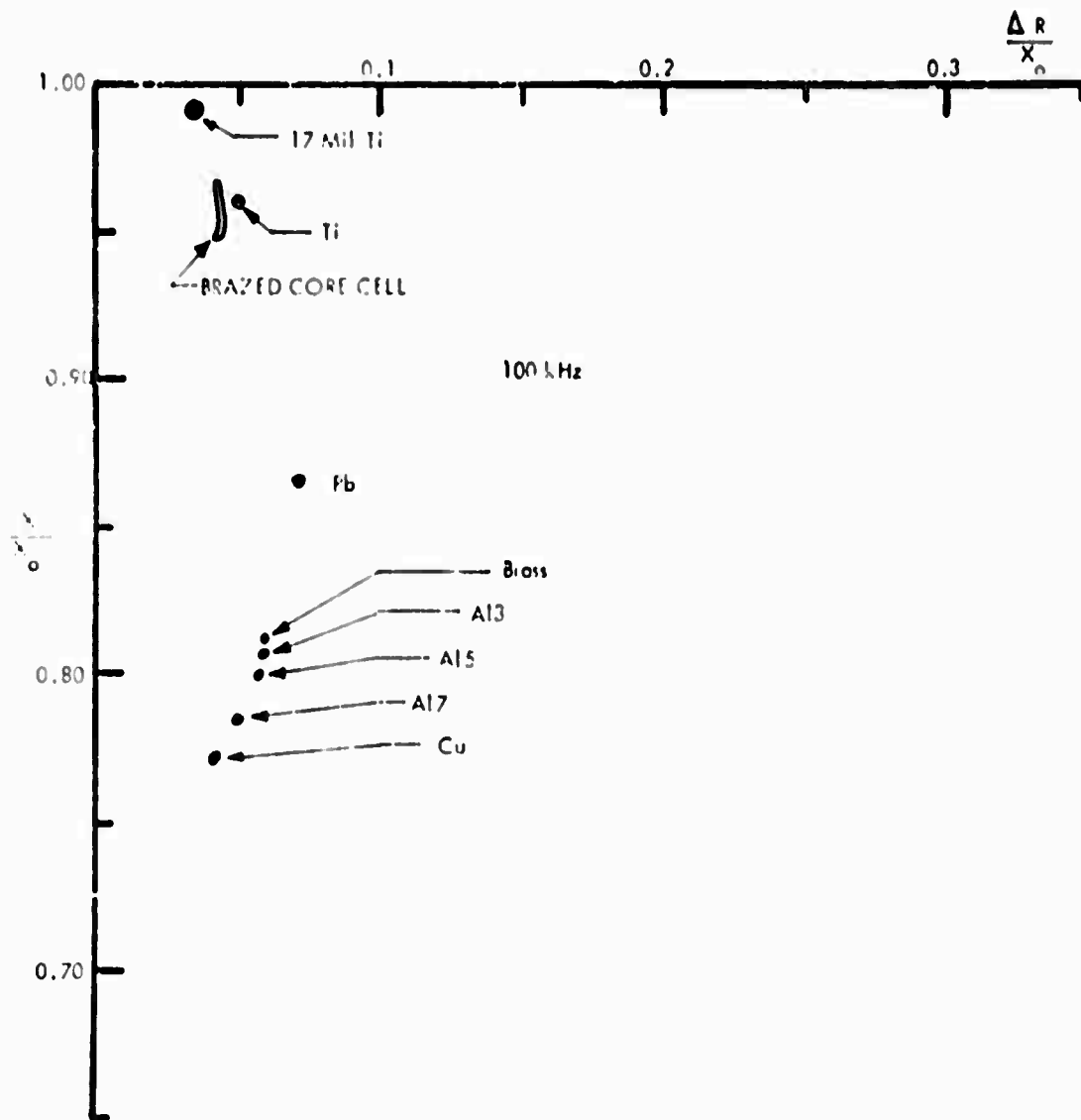


FIGURE 46 LOCATION IN IMPEDANCE PLANE OF EDDY CURRENT COIL SENSING ALUMINUM BRAZING MATERIAL IN TITANIUM HONEYCOMB TEST PART

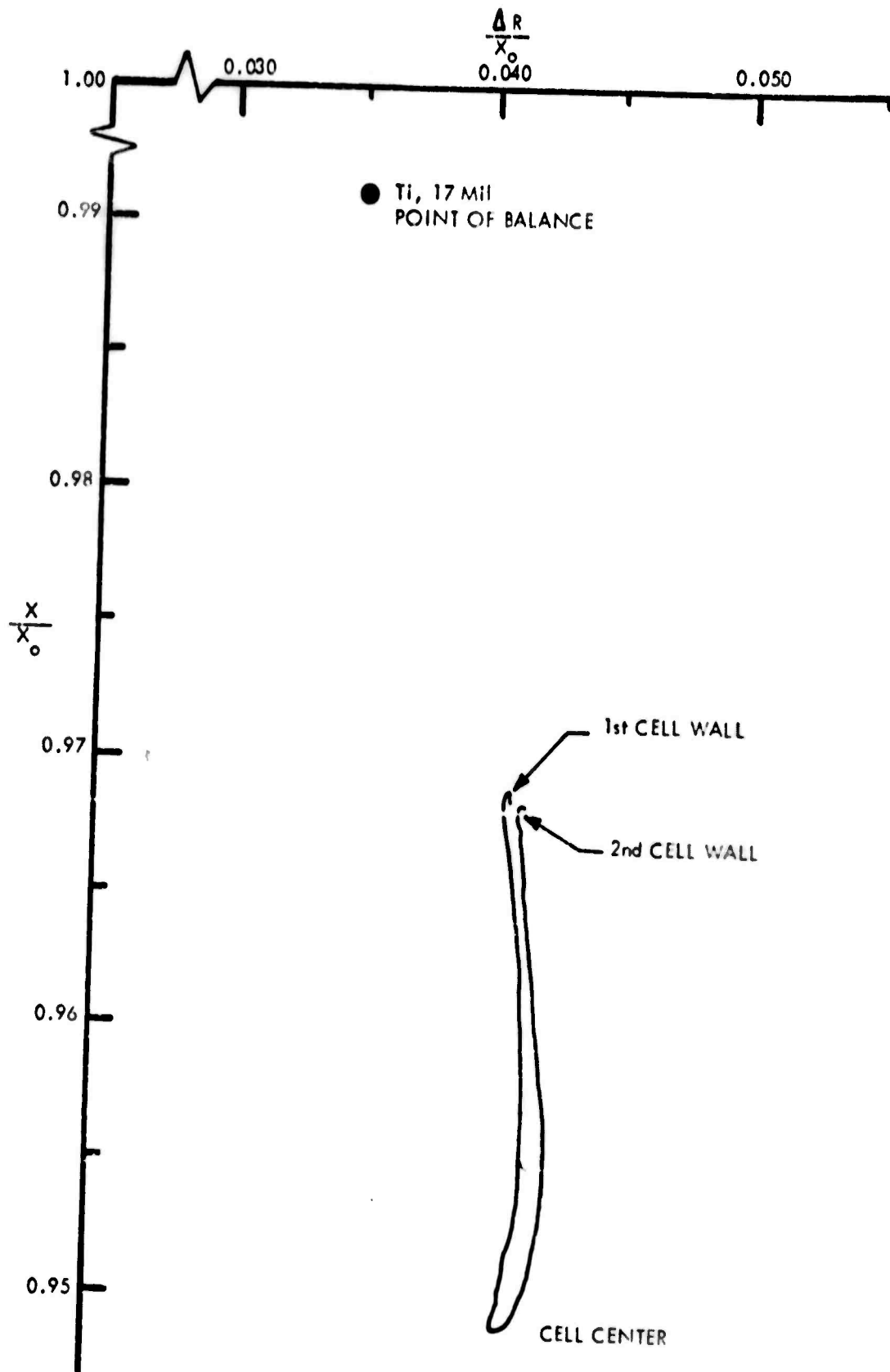


FIGURE 47 PASSAGE OF EDDY CURRENT COIL OVER CORE CELL OF AL BRAZED TITANIUM HONEYCOMB PANEL

impedance is located at the open end of the loop. When the coil center is located over a cell center the coil impedance is at the closed end of the loop. Figure 48 shows the effect of a change in face sheet thickness on the reaction of the eddy current coil. The single points represent the coil impedance when placed on bare titanium face sheet of the indicated thickness. These are the points upon which the NDT-3 is balanced when performing the actual inspection. As before, the loops represent the passage of the coil over the face of an actual brazed panel. These curves served as an assurance that it was valid to correct for face sheet thickness variations by merely readjusting the gain on the NDT-3. Figure 49 shows the reaction of the eddy current coil to differing amounts of aluminum brazing material. The upper loop is the coil response to passage over a cell on the upper surface of the panel where there appears to be less brazing material. The lower loop corresponds to a cell on the lower surface where more brazing material has accumulated. The various points shown indicate the coil impedance when located at a cell center for a number of representative cells.

Double Coil Tests

Theory

In a double coil eddy current probe one coil acts as transmitter and one as receiver. The probe may consist of a bifilar coil or two small coils wound separately and placed together. Under visual inspection it looks like a conventional single coil probe except that four leads extend from it. Electrically speaking, it is like a through transmission system in which both coils are placed on the same side. The major benefit of such a coil is insensitivity to temperature⁽⁹⁾. A double encircling coil system can, for instance, be used in the inspection of hot tubing. Temperature insensitivity is of value under normal temperature conditions when operating at high bridge balance. At high balance, coil temperature fluctuations can produce unacceptable resistive imbalance signals. In this laboratory high balance situations have been encountered in attempts to detect residual magnetization in ferrous specimens and in the inspection of low conductivity carbon fiber composites.

Quantitative data for double coil probes is not normally available. In this section, procedures are described for the collection and automatic recording of such data as the probe scans over the test part. The methods are analogous to those used for the collection of inductance and resistance data for single coil probes. Eddy current sensitivity is produced by the bridge balance method. For double coils one uses a mutual inductance bridge. Calibration is produced through the use of small mutual inductance plug-in modules. As in the case of through transmission eddy current systems the data is presented as a plot of V_{in}/V_o vs. V_{quad}/V_o .

Apparatus

The equipment for the collection of quantitative double coil eddy current data is pictured in Figure 50. The bridge supply and phase sensitive detection equipment is identical to that used for the single coil tests. Coherent cancellation is accomplished with the mutual inductance bridge shown in Figure 51. The important

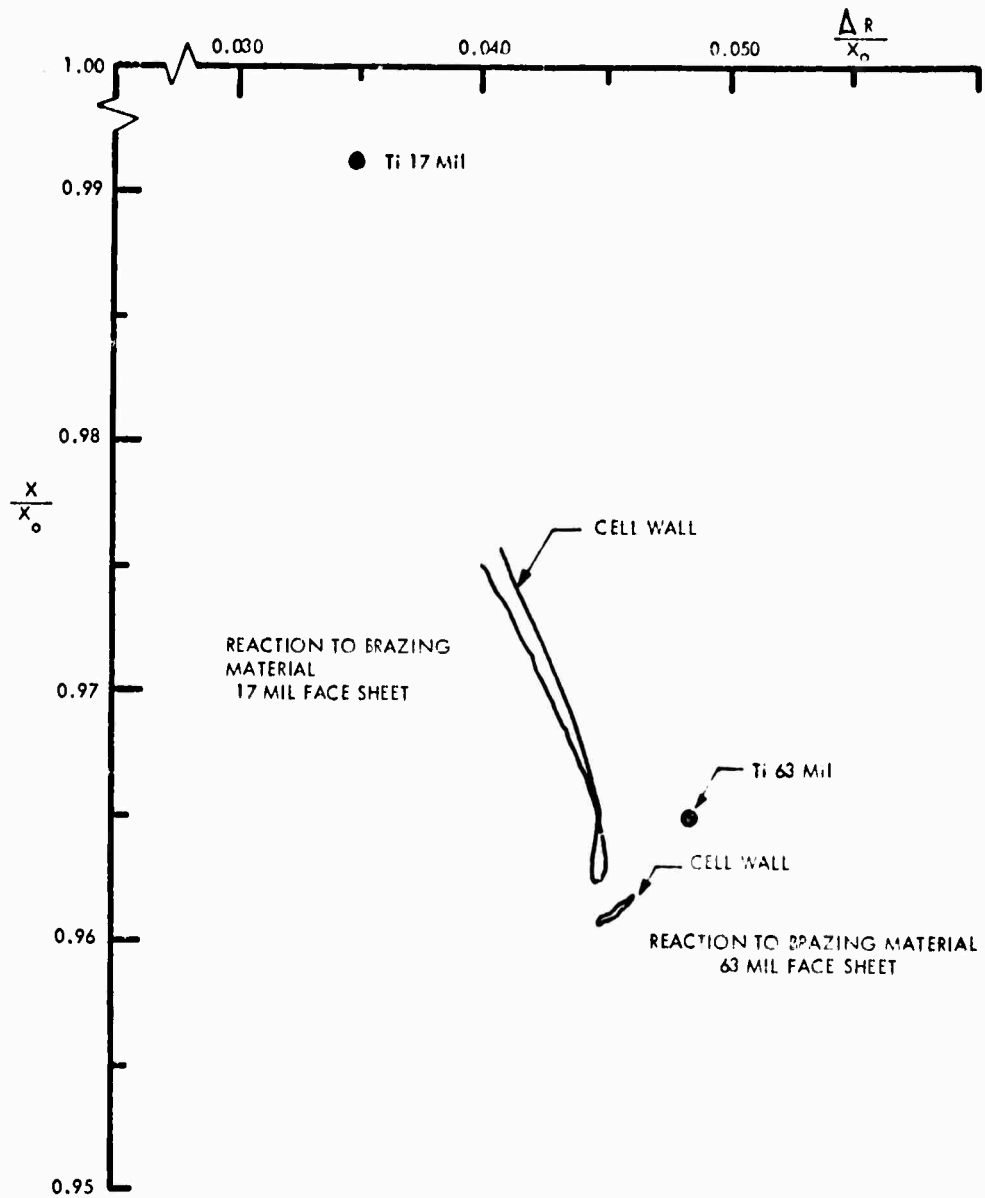


FIGURE 48 EFFECT OF CHANGE IN TITANIUM FACE SHEET THICKNESS

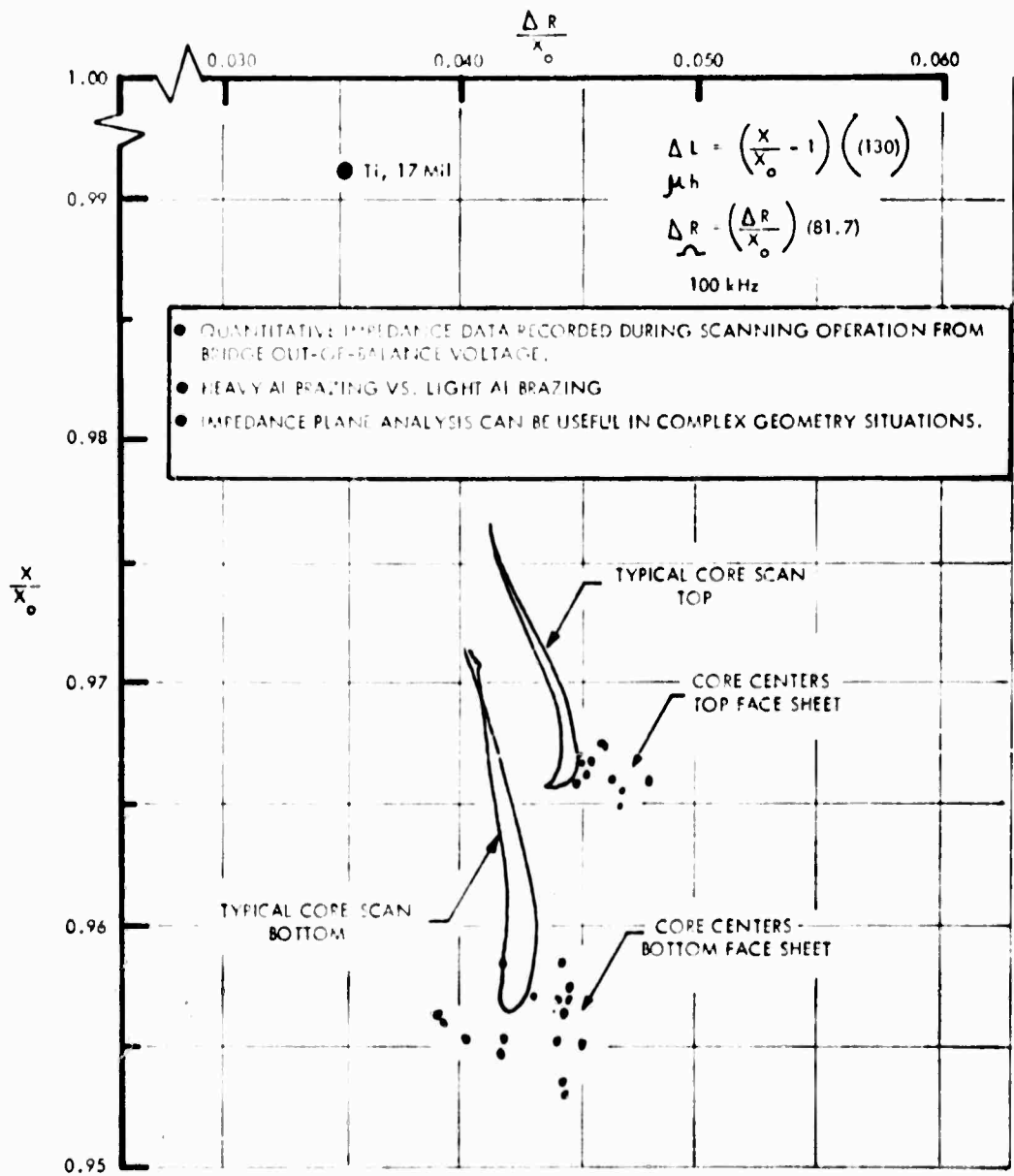


FIGURE 49 HEAVY Al BRAZING VS. LIGHT ALUMINUM BRAZING

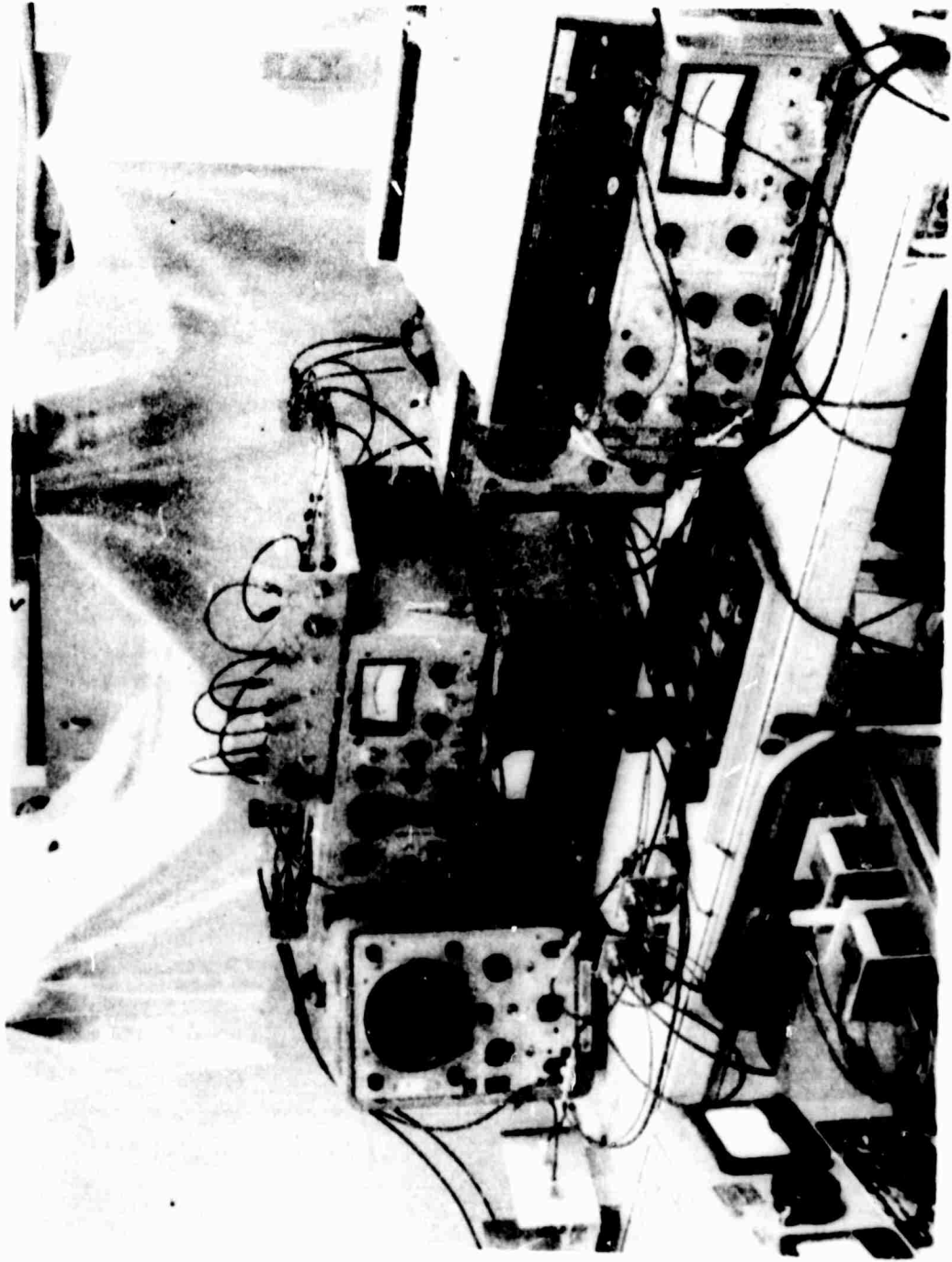


FIGURE 50 EQUIPMENT FOR COLLECTION OF QUANTITATIVE EDDY CURRENT DATA

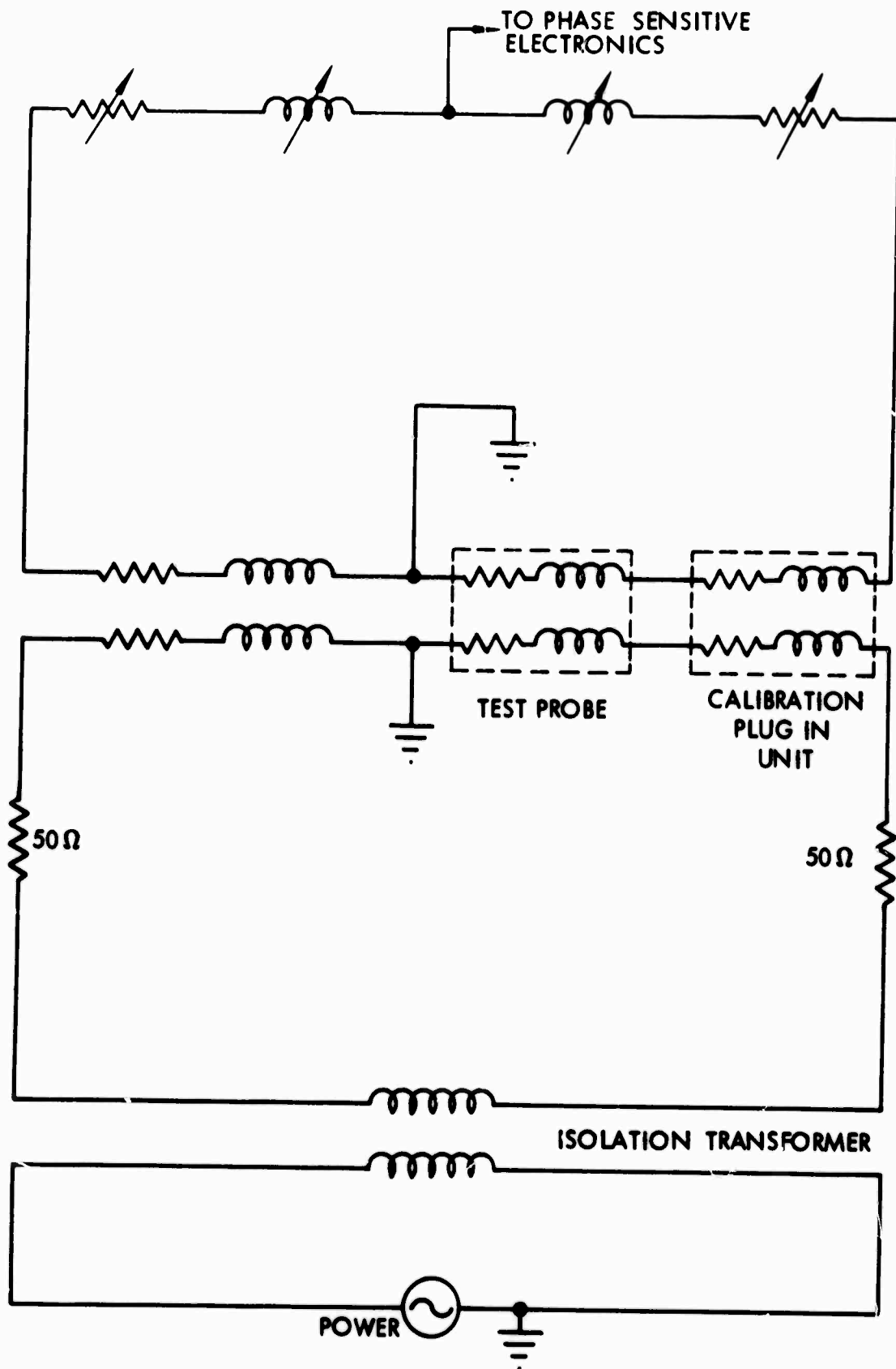


FIGURE 51 MUTUAL INDUCTANCE BRIDGE FOR CALIBRATED DOUBLE COIL EDDY CURRENT DATA

features of the bridge are the use of relatively high resistance pots for balancing and the inclusion of a mutual inductance plug-in unit for calibration purposes. Using this unit, the bridge can be checked, as before, to see that there is a linear relationship between bridge out-of-balance signal and mutual inductance changes in the probe.

The calibration procedure is exactly the same as it is for single coil tests. For the double coil case however, each plug-in unit is characterized by a particular value for V_{in}/V_o and V_{quad}/V_o . Before use of the modules for instrument calibration, these values have to be determined. The required measurements can be made using the mutual inductance bridge itself and lock-in amplifier. To perform these measurements, the test probe is removed, replaced by shorting wires, and the bridge is balanced. The probe is then inserted into the plug-in unit and the amplitude and phase of the bridge output determined. Comparing this to the amplitude and phase of the bridge output produced by each plug-in module produces the required numbers. As might be expected, the plug-in modules produce bridge outputs entirely in phase with V_o . The above sequence of steps is analogous to the determination of ΔR and ΔL for the single coil plug-in units by bridge balance methods. Once the mutual inductance plug-in units have been characterized by the above procedure the calibration of the instrument for actual use is precisely the same as it is for single coil tests.

The mutual inductance units are small transformers wound on cylindrical cores. The wire used was the same as that used for the probe coils and the cores are short pieces of wood doweling. There is no particular need to wind them with care as long as they are firmly mounted so that their electrical characteristics will not change. A little educated guessing will allow units to be wound which will vary in mutual inductance from about one percent to about fifty percent of a typical double coil probe. The precise electrical characteristics are then measured afterward using the methods discussed above.

Data and Conclusions

There is a continuing general interest in the identification of ferrous alloys and heat treat conditions using electromagnetic methods. One method frequently discussed involves the use of high frequency sensing in combination with a low frequency magnetic field bias. Studies in this laboratory have involved sensing impedance changes in eddy current coils during the application of an essentially DC magnetic field bias⁽¹⁰⁾. Quantitative data for this kind of test appears in the present section. The field coils, eddy current probe, and a typical test part used for the collection of such data appear in Figure 52.

The general location of ferrous and nonferrous metals in the voltage plane is shown in Figure 53. The appearance of this data is almost identical to the appearance of conventional impedance plane data. This is a strong indication that double coil systems are equivalent to single coil systems except for the added benefit of temperature insensitivity.



FIGURE 52 EDDY CURRENT PROBE ON FLAT IRON BAR BEING SUBJECTED TO D.C. MAGNETIZATION

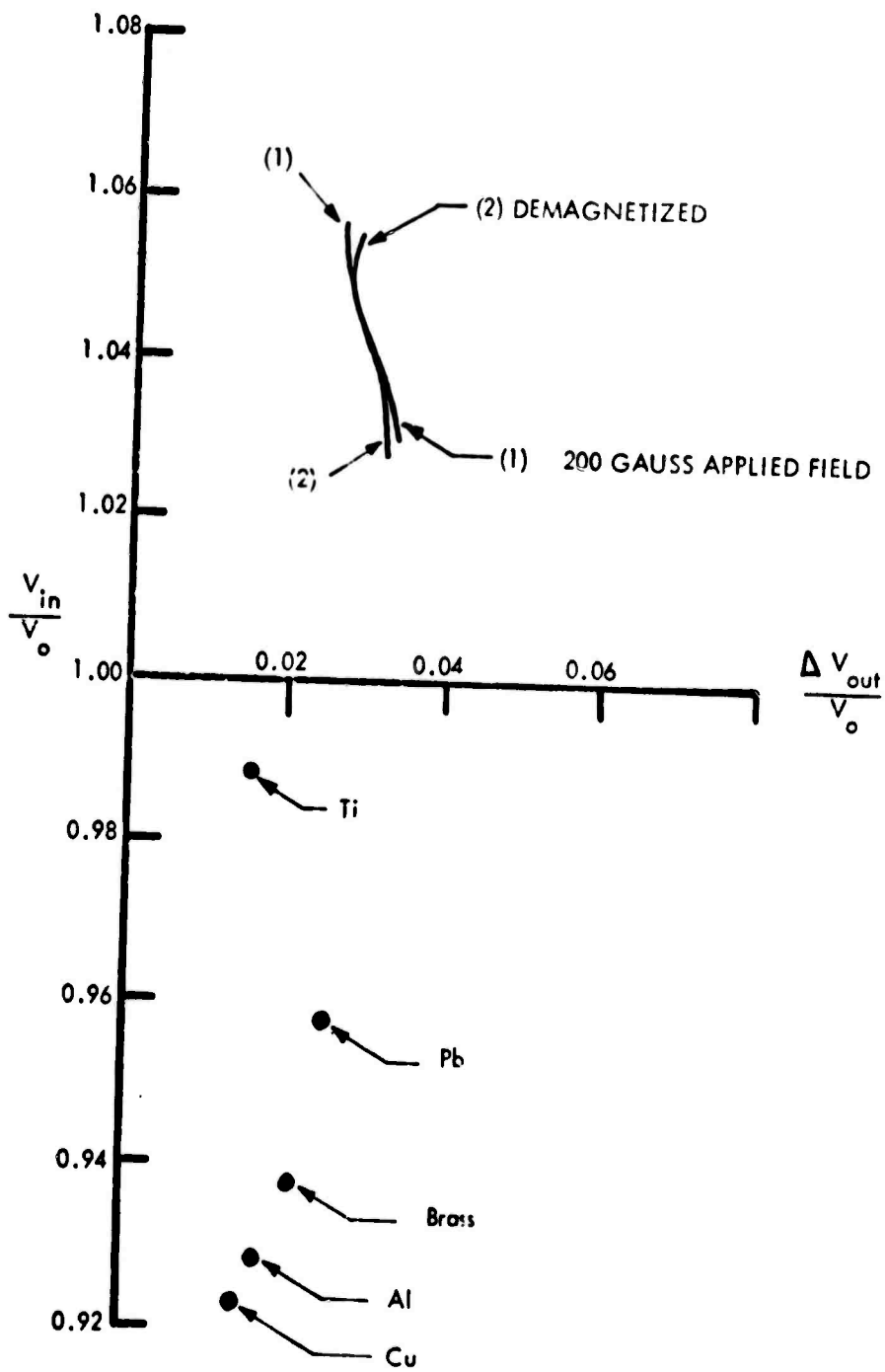


FIGURE 53 LOCATION OF FERROUS AND NONFERROUS METALS IN THE VOLTAGE PLANE

As the magnetic materials are slowly driven through a sequence of magnetic states the permeability changes. The resulting change in eddy current reaction for two different materials is described by the curves in the upper half of the diagram. These curves are not the result of a direct interaction between the test coils and the applied magnetic field. No such curves can be drawn by applying the magnetic field to an aluminum test bar. It is felt that the eddy current coil is sensing the actual change in magnetic state of the test part. Figure 54 is an expanded view of three test parts being subjected to DC magnetization. At the upper end of each narrow loop the part is demagnetized. As the part is magnetized, the pickup signal proceeds along the path shown. At the lower end of each loop the field is reversed and the part begins to move back toward its initial state. The existence of residual magnetism in the parts does not allow the eddy current reaction to return to the initial point, and the loops remain unclosed. The examination of eddy current reaction to residual magnetization requires greater amplification than is shown in this figure. Under these higher gain conditions the temperature insensitivity of the double coil probe should be useful

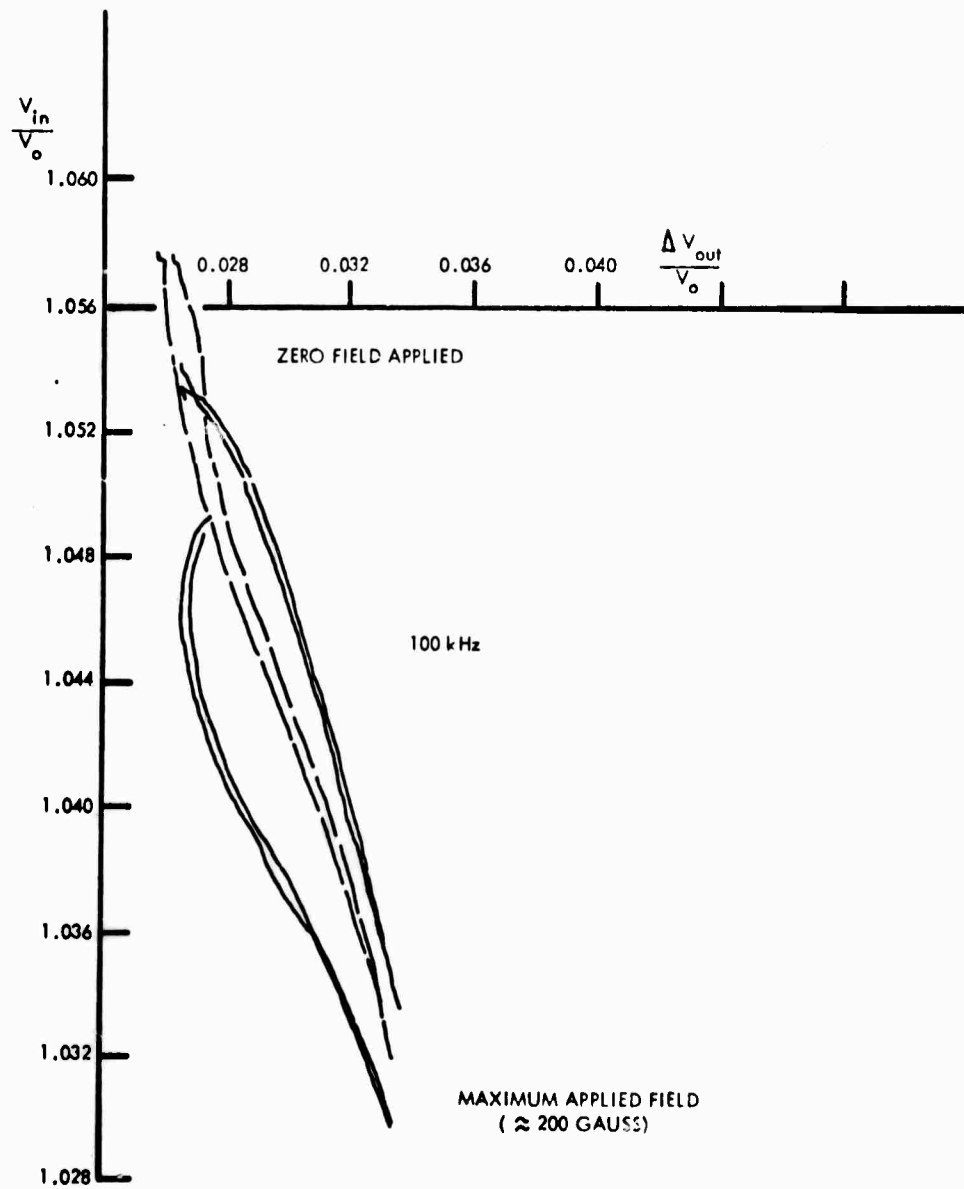


FIGURE 54 EDDY CURRENT REACTION TO THREE TYPES OF FERROUS FLAT BAR BEING SUBJECTED TO D. C. MAGNETIZATION

SUMMARY

In performing nondestructive tests to determine material properties or to detect imperfections in components or structures, the indications from conventional instruments are frequently of marginal value in enabling a decision to be made regarding the soundness of the test object. This may arise due to selection of non-optimized operating points, critical geometrical considerations in the test fixture, or noise may be a limiting factor in detecting the conditions of interest. The use of highly flexible signal processing instrumentation can frequently enable a detailed analysis of all of the information available in a given test and make possible the selection of optimum frequency and phase operating points at which tests may be most effectively performed.

In those tests in which random noise is a limiting factor, signal averaging may make a significant improvement in signal to noise ratios. Averaging may also be effective in reducing the effects of certain kinds of coherent noise. If the material conditions being measured have an appreciable length while the coherent noise sources are highly localized, signal averaging while scanning the material at a constant rate may result in improved detection of marginal defects. Reduced sensitivity to transducer positioning may also be obtained in some ultrasonic tests through application of signal averaging.

The use of appropriate means of display and recording of NDT data is quite important in providing the test operator with the information required to make decisions regarding material properties of interest. By providing several optional techniques of display and processing of the data from a given scan, the likelihood of successful detection of conditions harmful to the performance of a component or structure will be increased. Related to the problem of detecting and recording data is the concept of matched filtering. If undesirable material properties can be characterized in terms of their influence upon the nondestructive test signals, matched filtering will provide the optimum separation of wanted from unwanted signals. Since there are typically a wide variety of material conditions which must be detected in nondestructive testing problems, the flexibility of optical processing to achieve matched filtering is attractive.

FUTURE WORK

Refinements will be made in the system used for the photographic recording and reproduction of ultrasonic information. The techniques of optical band pass and matched filtering will be applied in an effort to enhance flaw signals and reduce coherent background noise. Attempts will be made to separate flaw information from background noise by recording gated ultrasonic information on magnetic tape and performing spectral analysis and autocorrelation on playback. Filter design will be considered. The use of a small digital computer for inspection control and data analysis will be examined. Efforts will be made to obtain a spectral and statistical characterization of the irregular signals obtained from ultrasonic grain boundary scattering. Both electrical and optical techniques will be examined.

BLANK PAGE

ACKNOWLEDGEMENTS

We thank Mr. Loyd George for electronic consultation and for designing and constructing eddy current coils. We also thank Mr. R. K. Vannier for aid in the design of ultrasonic experiments and for the careful collection of ultrasonic weld inspection data.

REFERENCES

1. J. C. Kennedy, W. E. Woodmansee, *Electronic Signal Processing Techniques-Phase I Final Report R-1933*, July 1969.
2. Data from Institute Dr. Foerster reported in *Nondestructive Testing Handbook*, R. C. McMaster, editor, Section 39, p. 15, Ronald Press, 1959.
3. *Nondestructive Testing Handbook*, R. C. McMaster, editor, Section 39, p. 13, Ronald Press, 1959.
4. J. D. Jackson, *Classical Electrodynamics*, p. 224, John Wiley and Sons, 1962.
5. J. C. Kennedy, W. E. Woodmansee, *Process Monitor for the Chemical Milling of SST Truss Core Material*, Boeing Report RSR-5543-5-7, March 1969.
6. W. E. Woodmansee, J. C. Kennedy, *Titanium Ribbon Thickness Measurements*, Boeing Report 2-5543-5000-226, January 1970.
7. J. C. Kennedy, W. E. Woodmansee, *Bolt Hole Crack Detection*, Boeing Report RSR-5543-5-8, February 1970.
8. W. E. Woodmansee, *Eddy Current Evaluation of Aluminum Brazed Titanium Honeycomb*, Boeing Report RSR-2-5543-2, May 1970.
9. C. V. Dodd, *Applications of a Phase Sensitive Eddy Current Instrument*, *Materials Evaluation*, 6, p. 260, 1964.
10. J. C. Kennedy, H. L. Southworth, *Investigation of Magnetic Flux Indicating Devices*, Boeing Report, March 1969.

DOCUMENT CONTROL DATA - R&D

(Security classification of title, body of abstract and indexing, and data must be entered when the overall report is classified.)

1. ORIGINATING ACTIVITY (Corporate author)		2a. REPORT SECURITY CLASSIFICATION	
The Boeing Company Aerospace Group Seattle, Washington 98124		UNCLASSIFIED	
2b. REPORT TITLE		2c. GROUP	
Electronic Signal Processing Techniques Phase II - Nondestructive Testing			
3. DATES COVERED (Type 1 - Report and include dates)			
Annual Report 30 October 1969 to 29 October 1970			
4. AUTHOR (or primary author) (Initial last name)			
James C. Kennedy Wayne E. Woodmansee			
5. REPORT DATE	7a. TOTAL NO. OF PAGES	7b. NO. OF REFS	
November 1970	81	10	
8. CONTRACT OR GRANT NO.		9a. ORIGINATOR'S REPORT NUMBERS	
DAAA 25-69-C0206 Project No. DA-W2-Z1246-F1-F6 AMCMS Code 5910.21.202891 ARPA Order No. 1246		The Boeing Company Report D180-10589-1	
		9b. OTHER REPORT NO(S) (Any other numbers that may be assigned this report)	
10. DISTRIBUTION STATEMENT			
Distribution of this document is unlimited.			
11. SUPPLEMENTARY NOTES		12. SPONSORING MILITARY ACTIVITY	
		Advanced Research Projects Agency (ARPA) Washington, D. C. Frankford Arsenal, Philadelphia, Pa.	
13. ABSTRACT			
Signal averaging was used to enhance flaw indications in the ultrasonic inspection of electron beam welds. An electronic gate, synchronized to the transducer motion through the use of an electrically controllable delay was also used to enhance flaw indications. To aid in electrical signal processing, a technique for recording ultrasonic video information on a low-frequency tape recorder was developed. In preparation for optical matched filtering, ultrasonic information was recorded on a photographic transparency in a C-scan format. An XY scanning densitometer was constructed to remove the intensity modulated information from the film and to aid in the production of hard copy recordings. Phaselock detection was used to perform through transmission eddy current testing. Methods were developed for obtaining quantitative through transmission data. Through transmission thickness measurements were performed and procedures were developed for obtaining a linear relationship between part thickness and eddy current signal. Applications to chemical milling and in-motion thickness measurements were demonstrated. Phaselock detection and signal averaging were used to measure resistance and inductance changes in conventional eddy current coils during a scanning operation. Quantitative data was produced from bridge unbalance signals. The data has the form X/X_0 vs. $\Delta R/X_0$. An application to aluminum brazed titanium honeycomb was examined. Phaselock detection and signal averaging were used to produce quantitative data in two coil eddy current systems. The data has the form V_{in}/V_0 vs. $V/\text{quad}/V_0$. An application to the inspection of ferrous materials was examined.			

2	P E R A M	S E P 15		S E P 15	
		A	A	A	A
Nondestructive Testing Data Processing Data Analysis Pattern Recognition Correlation Digital Computer Diagnostic Equipment Flaw Detection Acoustic Analysis Statistical Analysis Signature Analysis Materials Evaluation Eddy Current Testing Ultrasonic Testing Optical Signal Processing					